Journal of Hazardous Materials 487 (2025) 137257

Contents lists available at ScienceDirect

Journal of Hazardous Materials

journal homepage: www.elsevier.com/locate/jhazmat

Interleukin-33 modulates NET formation via an autophagy-dependent manner to promote neutrophilic inflammation in cigarette smoke-exposure asthma

Jing Liu [1], Peizhi Tao [1], Beiting Su [1], Li Zheng, Yusen Lin, Xiaoling Zou, Hailing Yang, Wenbin Wu, Tiantuo Zhang [*,2], Hongtao Li [*,3]

Department of Pulmonary and Critical Care Medicine, The Third Affiliated Hospital of Sun Yat--sen University, Institute of Respiratory Diseases of Sun Yat--sen University, Guangzhou, PR China

HIGHLIGHTS

- Cigarette smoke exposure leads to a neutrophil--related phenotype in asthma.
- IL-33 accentuates Th2/Th17 related inflammation in cigarette smoke-exposure asthma.
- IL-33 stimulates NET formation, resulting in enhanced neutrophilic inflammation.
- Feedforward connection between NET formation and neutrophil autophagy.

GRAPHICAL ABSTRACT

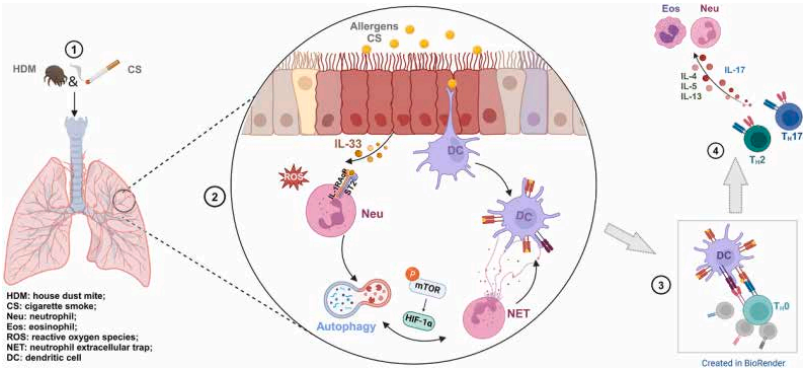

ARTICLE INFO

Keywords:
Cigarette smoke
Non--T2 asthma
Interleukin-33
Neutrophil extracellular traps
Autophagy

ABSTRACT

Cigarette smoke (CS) contributes to IL---33 release and neutrophil inflammation in asthma. Neutrophil extracellular traps (NETs) are essential for neutrophil function. However, the effect of IL--33 on neutrophils in cigarette smoke--exposure asthma remains unclear. We found that CS exposure led to lower lung function and a neutrophil--related phenotype in asthma, characterized by elevated neutrophil and Th17 cell counts. Granulocytic airway inflammation was ablated by sST2, which blocked excessive IL--33 release. Transcriptome analysis of mouse lungs revealed that IL--33 enhanced NET formation in HDM/CS-treated mice, which was further

Abbreviations: CS, cigarette smoke; CSE, cigarette smoke extract; HDM, house dust mite; BALF, bronchoalveolar lavage fluid; AHR, airway hyperreactivity; WT, wild type; IL--33 KO, IL--33 knockout; sST2, IL--33 receptor; HRP, horseradish peroxidase; ROS, reactive oxygen species; NAC, N--Acetyl--L--cysteine; PBMCs, peripheral blood mononuclear cells; PBN, peripheral blood neutrophil; DCs, dendritic cells; PMA, phorbol 12--myristate 13--acetate; GM--CSF, granulocyte--macrophage colony stimulating factor; NETs, neutrophil extracellular traps; mTOR, mammalian target of rapamycin.

* Corresponding authors.
E-mail addresses: zhttuo@mail.sysu.edu.cn (T. Zhang), lihongt2@mail.sysu.edu.cn (H. Li).
[1] These authors contributed equally to this work.
[2] ORCID: 0000-0002-9239-0434
[3] ORCID: 0000-0002-3337-483X

https://doi.org/10.1016/j.jhazmat.2025.137257
Received 20 July 2024; Received in revised form 3 January 2025; Accepted 15 January 2025
Available online 16 January 2025

confirmed in our experimental asthma model and in asthma patients. NETs were associated with poor lung function and airway inflammation and directly facilitated monocyte--derived dendritic cell activation, further inducing Th2/Th17 polarization. Furthermore, we demonstrated a feedforward loop between NETs and neutrophil autophagy, both of which are dependent on reactive oxygen species (ROS) production and the mTOR-Hif-1α signaling pathway. Notably, IL--33 knockout suppressed autophagy and NETs, whereas the autophagy agonist rapamycin reversed the inhibition of NETs by sST2 in a mTOR--dependent manner. Our findings revealed that the IL--33/ST2 signaling pathway interacts with the neutrophil -autophagy--mTOR-Hif-1α-NET pathway, ultimately aggravating Th2/Th17-related inflammation. These insights could lead to potential therapeutic targets for mitigating exacerbations in asthmatic patients who are exposed to CS.

1. Introduction

Asthma is a complex heterogeneous disease resulting from the interactions of genes and the environment.[1] Current smoking status correlates with neutrophilic airway inflammation.[2,3] Cigarette smoke (CS) exposure triggers oxidative stress,[4] leading to the release of proinflammatory cytokines from activated neutrophils, macrophages, $CD8^+$ T cells, and type 3 innate lymphoid cells (ILC3s).[5–7] These inflammatory responses contribute to non--T2 airway inflammation as well as epithelial and other structural damage.[8] Furthermore, multiple observational studies have demonstrated a link between current smoking status and worsened clinical outcomes in patients with asthma.[9] Increased cumulative exposure to CS is also related to worsening asthma control.[10]

Activated neutrophils stimulated by infectious or noninfectious mediators can release neutrophil extracellular traps (NETs), which include neutrophil proteases, myeloperoxidase (MPO), histones, and double-stranded DNA (dsDNA), thereby inducing inflammation and damage.[11,12] NETs have been observed in the airways and mediastinal lymph nodes of patients with asthma during both T2 and non--T2 immune responses.[13] A recent study revealed that high levels of extracellular DNA (eDNA) in sputum were related to poor asthma management and mucus overproduction.[14] Collectively, these findings indicate that dysregulation of NETs may contribute to asthma pathobiology, even though the mechanisms involved in NET formation are not well known. Autophagy has been suggested to have a positive effect on the formation of NETs.[15] Activating of autophagy, such as by inhibiting mammalian target of rapamycin (mTOR) with rapamycin, enhances NET production,[16] while reducing autophagy decreases NET release.[17] Understanding the association between neutrophil autophagy and NETs may be essential for obtaining insights into the pathophysiology of neutrophilic asthma.

Several environmental factors (e.g., pathogens and CS) have been found to initiate the secretion of epithelium--derived alarmins (i.e., IL--33, thymic stromal lymphopoietin, and IL--25), which are involved in both innate and adaptive immune responses in T2 and non--T2 asthma patients.[18,19] We previously revealed that epithelium--derived IL--33 acts as a proinflammatory cytokine to modulate Th2/Th17--related airway inflammation in cigarette smoke--exposure asthma.[20,21] Studies have also shown that IL--33 activates neutrophils to produce reactive oxygen species (ROS) and NETs in cutaneous infection and bronchopulmonary dysplasia,[22–24] and that NETs can damage the integrity of the bronchial epithelium, resulting in the release of IL--33 and increased airway inflammation.[25] However, additional evidence is needed to determine the mechanism by which IL--33 is involved in innate and adaptive immune responses in cigarette smoke--exposure asthma.

In the present study, we found that CS leads to neutrophil--related airway inflammation in asthma through the release of IL--33. Elevated IL--33 activates neutrophils to produce NETs, which are connected with autophagy through the mTOR-Hif-1α pathway, facilitating dendritic cell (DC) activation and Th2/Th17 immune response. Here, we present evidence for the mechanism of neutrophilic lung damage and open the door to potential specific biologicals for non--T2 cigarette smoke-exposure-related asthma.

2. Materials and methods

Detailed descriptions of the methods used are available in the online supplementary material.

2.1. Cigarette smoke--exposure asthma mouse model

Twenty-four female C57BL/6 J mice (6--8 weeks old) were classified into four groups: the Con group, composed of unsensitized mice that received intraperitoneal (i.p.) injection and intranasal (i.n.) instillation of PBS; the CS group; the house dust mite (HDM) group; and the HDM/CS group (n = 6/group). Chronic asthma models were generated as previously described.[26] Briefly, the HDM group and HDM/CS group were sensitized through i.p. injection of 20 μg of HDM (the most important allergen of allergic asthma; XPB82D3A2.5; Greer Laboratories, USA) combined with 100 μL of alum adjuvant (77161; Thermo Fisher Scientific, USA) in 100 μL of PBS on Days 0 and 14, respectively. The mice were further challenged by i.n. inhalation of 10 μg of HDM in 30 μL of PBS three times per week for 6 weeks. In the protocol for exposure to CS, the mice in the CS group and HDM/CS group were exposed to 6 cigarettes with the filters removed for a period of approximately 30 min, twice daily for 5 days/week during HDM challenge. The other two groups were exposed to room air. At the end of the 9th week, the mice were anesthetized and sacrificed. Bronchoalveolar lavage fluid (BALF), serum, lung, and spleen specimens were collected for further study. All mice were purchased from GemPharmatech Co., Ltd.

2.2. In vivo IL--33 neutralization and CRISPR--Cas9--mediated gene knockout

To prophylactically block the effects of IL--33, mice were intraperitoneally injected with 1 μg of recombinant mouse sST2 (CK89, Novo-Protein, China) in PBS 30 min prior to HDM challenge.[27] In addition, IL--33 knockout mice (IL-33 KO) were constructed using CRISP-R--Cas--mediated genome engineering technology by Cyagen Biosciences (Guangzhou, China).

2.3. In vivo intervention in NET formation

In some experiments, mice were injected i.p. with 5 mg/kg Cl--amidine (PAD inhibitor; HY--100574 A, MCE, USA) 30 min before HDM challenge. As a positive control for NET formation, mice were administered i.p. injections of 200 μg/kg phorbol 12--myristate 13--acetate (PMA; HY--18739, MCE, USA) 30 min before the last two HDM challenges.[28]

2.4. In vivo autophagy inhibitor, 3--MA administration

To investigate the participation of autophagy in asthma, mice were administered 3--methyladenine (3--MA, 15 mg/kg; M9281, Sigma--Aldrich, USA) via i.p. injection 30 min before every single challenge.

[29] In some cases, we used the autophagy agonist rapamycin (2 mg/kg; HY--10219, MCE, USA) intraperitoneally twice during the last week of challenge.[30] Control mice were intraperitoneally injected with PBS.

2.5. RNA preparation and sequencing

Total RNA was extracted from mouse lungs (n = 3/group). The sequencing library was prepared following the instructions of the TruSeqTM RNA Sample Prep Kit (Illumina, San Diego, CA). The paired--end RNA library was sequenced with the Illumina NovaSeq 6000 sequencing platform (2 × 150 bp read length).

2.6. Transcriptomic bioinformatic analysis

The RNA sequencing (RNA-seq) data were deposited in NCBI's SRA (PRJNA1073012) and processed online on the Majorbio Cloud Platform (www.majorbio.com). Briefly, the quality of the RNA-seq data was evaluated by fastp.[31] RNA--seq reads were subsequently aligned to the reference genome (GRCm39 from the *Mus musculus* genome) using HISAT2 software and assembled with StringTie.[32] A total of 31,004 genes were subjected to differential expression gene (DEG) identification, clustering, functional enrichment, and weighted gene coexpression network analysis (WGCNA). The expression level of each transcript was calculated according to the transcripts per million reads (TPM) method. RSEM[33] was used to quantify gene abundances and perform principal component analysis (PCA; the first two principal components were drawn). Essentially, DEGs were identified using DESeq2.[34] GO enrichment and KEGG pathway analyses were performed by Goatools and KOBAS, respectively.[35] WGCNA[36] was used to identify gene modules associated with the effects of IL--33 on cigarette smoke--exposure asthmatic mice.

2.7. Details of the clinical samples

We recruited 10 healthy control participants (never smoked), 15 asthma patients (never smoked), and 14 asthma smokers (current smoking). All subjects provided written informed consent. More details on the preparation of serum, peripheral blood neutrophils (PBN), monocyte--derived DCs, and naive $CD4^+$ T cells are available in the online supplementary methods and Fig. S1.

2.8. Preparation of HDM and cigarette smoke extract (CSE)-induced NETs and stimulation of DCs

To determine the effect of HDM/CSE--induced NETs on DCs, freshly isolated neutrophils from healthy donors were stimulated with HDM (0.5 μg/mL Der p 1, the main allergen of HDM; XPB91D3A2.5, Greer, USA) and 2 % CSE for 24 h. In some experiments, HDM alone was used as a control. The supernatant was then aspirated, the plate was gently washed with PBS to remove the stimulus, and QuickCut™ AluI (1603, TAKARA, Japan) was added to obtain cell--free eDNA. The concentration of NETs was detected using a NanoDrop spectrophotometer. The DCs were stimulated with HDM or HDM/CSE--induced NETs (20 ng/mL) for 24 h.[37] IFN--γ (10 ng/mL; CI57, NovoProtein, China) was used as a positive control. Subsequently, CD11c (PE; 301605, Biolegend, USA), CD40 (APC; 334309, Biolegend, USA), and CD86 (APC; 305411, Biolegend, USA) expression on the surface of the DCs was determined via flow cytometry.

2.9. Coculture of DCs with naive $CD4^+$ T cells

To assess the capacity of NET--induced DCs to promote naive $CD4^+$ T lymphocyte differentiation, on Day 5, the DCs were treated with IFN--γ (10 ng/mL) for 24 h, with or without NETs. Then, the DCs were cocultured with human naive $CD4^+$ T cells from healthy donors at a ratio of 1:5 DC/T--cell in medium containing 25 μL/mL CD3/CD28 (10971, Stemcell, Canada) and 10 ng/mL IL--2 (C013, NovoProtein, China) for 4 days. The cells were primed with 50 ng/mL PMA (HY--18739, MCE, USA), 1 μg/mL ionomycin (70--CS0002, MultiSciences, China), and 1.5 μL/mL protein transport inhibitor (554724, BD, USA) for 5 h. The cells were subsequently stained for CD4 (FITC; 317407, Biolegend, USA), IL--13 (PE; 501903, Biolegend, USA), and IL--17 A (APC; 512333, Biolegend, USA) which were subsequently analyzed via flow cytometry. [37]

2.10. Statistical analysis

The data are shown as the mean ± SEM. A t--test was used to compare the data between two groups. The data from more than two groups were subjected to analysis of variance (ANOVA) with Tukey's correction for multiple comparisons. P values < 0.05 were regarded as significant. All the statistical analyses were conducted using GraphPad Prism 8.0 (San Diego, CA).

3. Results

3.1. Cigarette smoke exposure leads to poor lung function and a neutrophil--related phenotype in asthma

The clinical information is summarized in Table S1. We found that asthma patients (both never smokers and current smokers) had higher levels of eosinophil counts in peripheral blood compared to healthy controls. Additionally, asthma smokers showed higher levels of total IgE and neutrophil counts than healthy controls, as well as poorer lung function (FEV_1/predicted value and FEV_1/FVC) than asthmatics (never smoked) and healthy individuals. To further determine the detrimental effects of CS on asthma inflammatory phenotypes, we first established a HDM--induced chronic asthma mouse model according to the protocol shown in Fig. 1A. This mouse model exhibited increased AHR (Fig. 1B), peribronchial inflammation, mucus secretion, and subepithelial collagen deposition (Fig. 1C); eosinophils and macrophages in BALF (Fig. 1D and E); and eosinophils in the lung (Fig. 1F and G) and spleen (Fig. S2), as compared with the control group. Subsequently, cigarette smoke exposure was performed in our HDM--induced mouse model (Fig. 1A), which resulted in more severe airway inflammation, especially neutrophilic inflammation, than HDM treatment alone. This was manifested by exacerbated inflammatory cell infiltration, goblet cell hyperplasia, and airway remodeling (Fig. 1C), with a marked increase in neutrophils in the BALF (Fig. 1D and E), lung (Fig. 1F and G), and spleen (Fig. S2).

We also observed the costimulatory molecules CD40 and CD86 on DCs as well as Th2, Th17, and Th1 cells in the mouse lung and spleen. In addition, DCs in the lungs (Fig. 1H) and spleens (Fig. S3) of HDM/CS--treated mice exhibited a more activated phenotype with elevated CD40 and CD86 expression compared to the control group. Moreover, Th2 cells in the lung (Fig. 1I) and spleen (Fig. S4) were more prominent in HDM--induced asthmatic mice than in vehicle- and CS-treated controls; however, additional CS exposure led to increased Th17 cell differentiation compared to HDM treatment alone. The same results were observed in the serum of asthma patients. Active smoking of asthmatics has been attributed to overproduction of IL-17 A compared with elevated type 2 cytokine IL-4 alone in nonsmoking asthmatics (Fig. 1J and K).

We further performed whole-transcriptome RNA sequencing on the lung tissues of HDM/CS--treated mice and control mice (n = 3/group) to validate our *in vivo* results. Principal component analysis (PCA) revealed clear segregation of the transcriptional programs between the HDM/CS group and the control group (Fig. 2A). We identified 446 DEGs, 377 of which were upregulated and 69 of which were downregulated (Fig. 2B and Table S3). GO (Fig. 2C) and KEGG (Fig. 2D) pathway analyses of the 446 DEGs revealed that genes associated with neutrophil chemotaxis and migration, the inflammatory response, the immune response, and

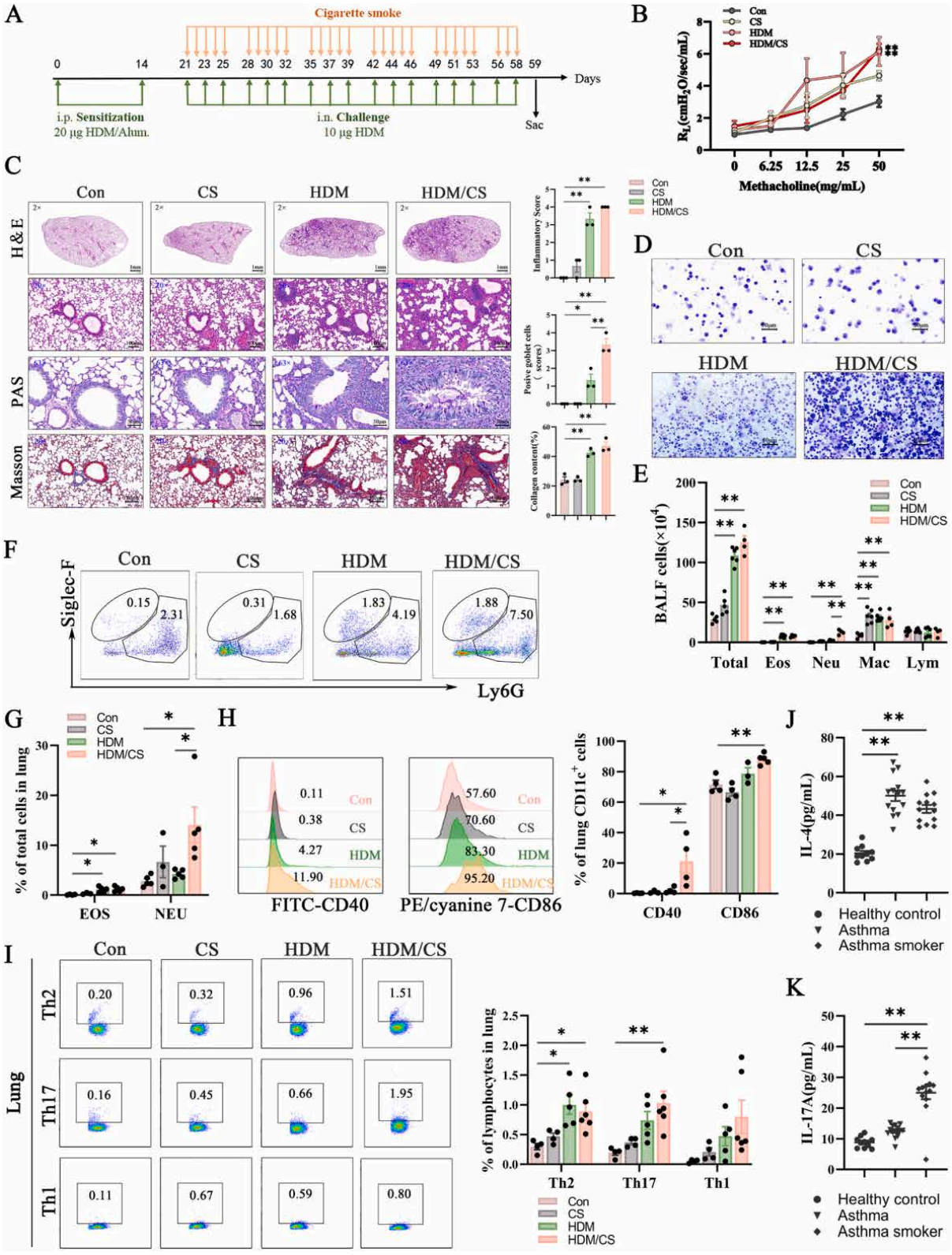

Fig. 1. In asthma, CS exacerbates neutrophilic AHR, airway inflammation, DC activation, and Th2/Th17 responses. A Experimental timeline for the cigarette smoke--exposure asthma mouse model. B Lung resistance (R_L) was determined in response to increasing concentrations (0, 6.25, 12.5, 25, and 50 mg/mL) of methacholine (n = 3). C Histological mouse lung sections stained with H&E (scale bars, 1 mm for 2x magnification and 100 μm for 20x magnification), PAS (scale bars, 50 μm), and masson (scale bars, 100 μm) (n = 3). D Diff--quick staining of BALF (scale bars, 50 μm). E Cellular classification (Eos, eosinophil; Neu, neutrophil; Mac, macrophage; Lym, lymphocyte) of BALF (n = 4–6). F and G Eosinophils ($CD45^+CD11c^{low}CD11b^+SiglecF^+$) and neutrophils ($CD45^+CD11c^{low}CD11b^+Ly6G^+$) in mouse lungs were evaluated via flow cytometry (n = 3–5). H Matured DCs ($CD45^+CD11c^+CD40^+$ and $CD45^+CD11c^+CD86^+$ cells) in mouse lungs were detected through flow cytometry (n = 3–5). I Th2 ($CD4^+IL\text{--}4^+$), Th17 ($CD4^+IL\text{--}17\ A^+$), and Th1 ($CD4^+IFN\text{--}\gamma^+$) cells in the mouse lung (n = 4–6). J and K Concentrations of IL--4 (J) and IL--17 A (K) in serum from asthma smokers (n = 14), asthma patients (n = 13), and healthy controls (n = 10) determined via ELISA. The data are presented as the mean ± SEM. $^*P < 0.05$; * $^*P < 0.01$.

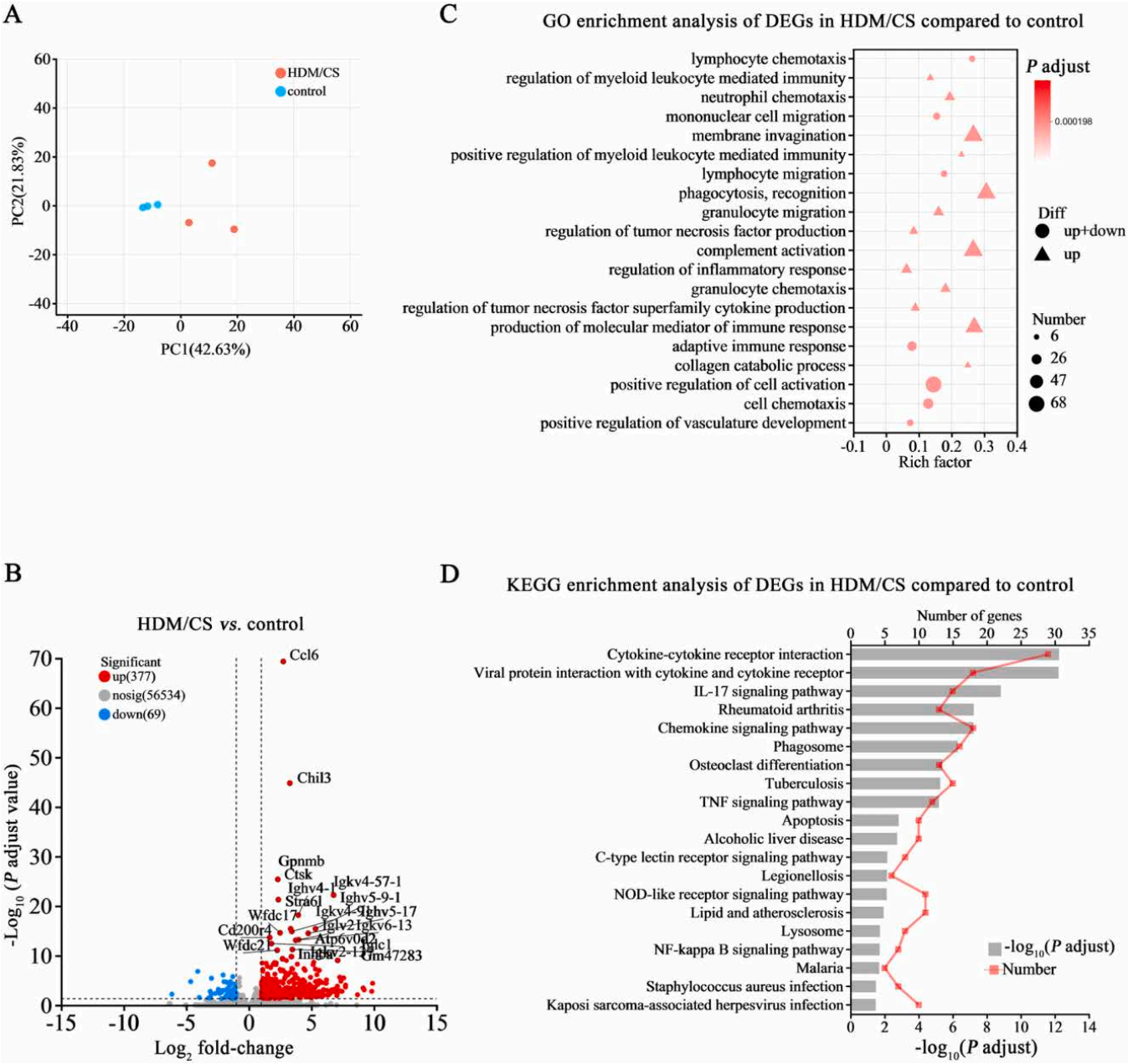

Fig. 2. The neutrophil--related gene pathways are related to cigarette smoke--exposure asthma. A Similarity of gene expression profiles from lung tissues between HDM/CS (n = 3, red circle) and control (n = 3, blue circle) mice determined by PCA. B Volcano plot depicting the results of DEG analysis between HDM/CS and controls. *P* value < 0.05 & $|\log_2$ (fold--change)| > 1. C GO enrichment analysis of 466 DEGs in the HDM/CS vs. control groups. The top 20 enriched GO terms are listed according to the *P* value (y-axis). The X-axis indicates the enrichment factor. The bubble color indicates the adjusted *P* value and the bubble radius indicates the number of genes. D KEGG pathway analysis of DEGs. The top 20 enriched biological functions are presented on the basis of the *P* value (y-axis). The x-axis indicates the $-\log_{10}$ adjusted *P* value. The number represents the number of genes.

the IL--17 signaling pathway were significantly upregulated in HDM/CS--treated mice. These findings indicated a strong association between cigarette smoke exposure and neutrophil-related responses.

3.2. Excessive IL--33 contributes to mixed granulocytic airway inflammation in mice

We previously identified a potential proinflammatory role for IL--33 in cigarette smoke--exposure asthma.[20,21] Here, we found a considerable amount of IL--33 in the serum of asthmatic patients (both never smokers and current smokers) and in our cigarette smoke--exposure asthma model both *in vitro* and *in vivo* (Fig. 3A--D). We used recombinant mouse sST2 (the IL--33 receptor, a negative regulator of IL--33 activity) to ascertain the role of IL--33 in cigarette smoke--exposure asthmatic mice (Fig. 3E). Our results showed that blockade of IL--33 reduced the intensity of AHR (Fig. 3F), the thickness of the bronchial inflammatory cell layer, and the percentage of the mucus--covered area (Fig. 3G). The numbers of neutrophils and eosinophils in the BALF (Fig. 3H), lung and spleen (Fig. 3I and Fig. S5) were also notably lower. In addition, compared with HDM/CS treatment alone, sST2 treatment abrogated the expression of CD40 and CD86 on DCs in the spleen (Fig. 3J and Fig. S6A) as well as the proportions of Th2 and Th17 cells in the lung and spleen (Fig. 3K--N and Fig. S6B and C).

RNA sequencing of lung tissues from sST2--treated mice revealed differences according to PCA of the gene expression profiles (Fig. S7A). A total of 341 DEGs were detected in the HDM/CS/sST2 and HDM/CS

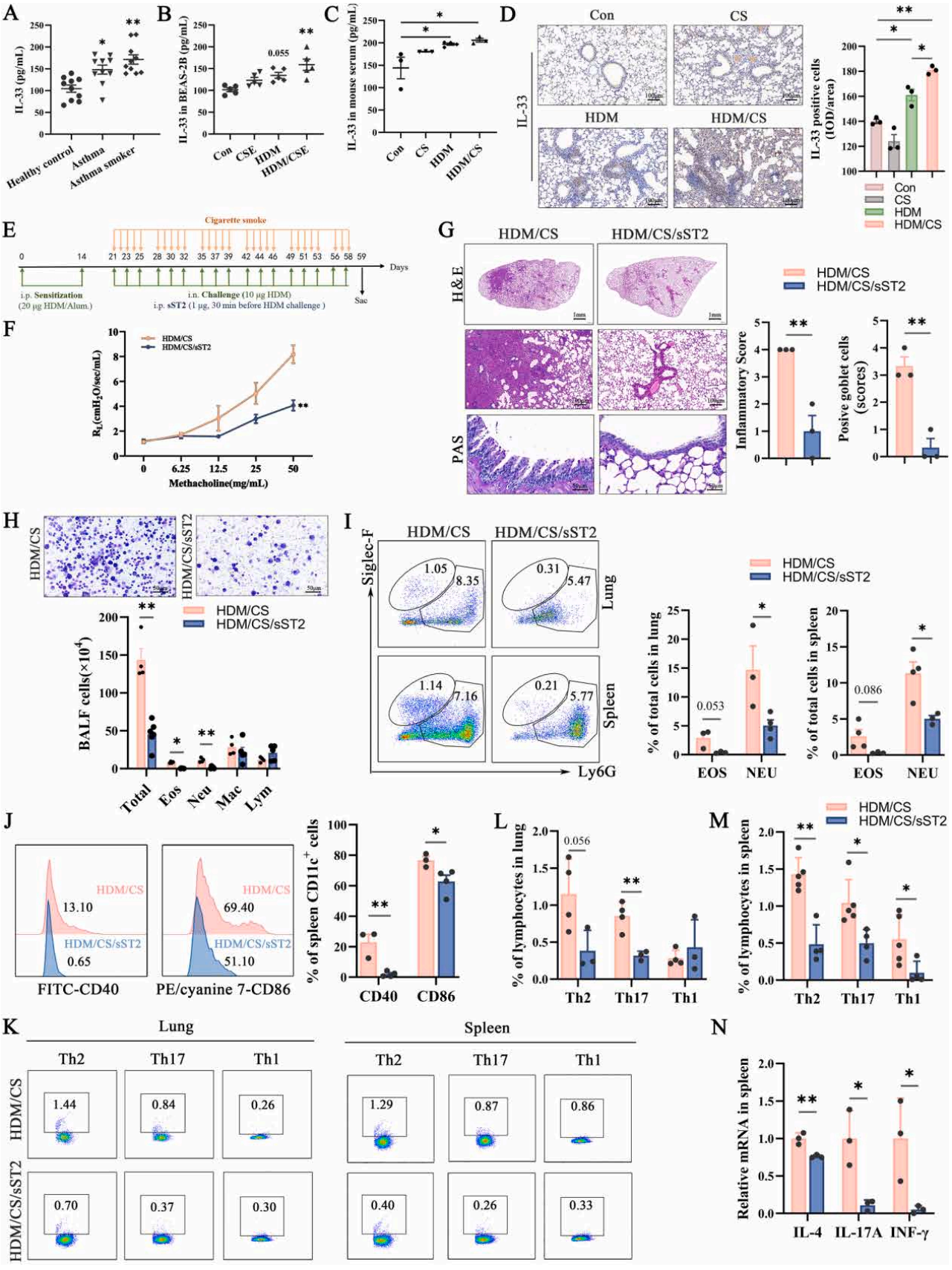

(caption on next page)

Fig. 3. Excessive IL--33 contributes to Th2/Th17 responses and neutrophilic inflammation. A Serum IL--33 levels in asthma smokers, asthma patients, and healthy controls (n = 10/group) determined via ELISA. B IL--33 in the supernatant of BEAS--2B cells treated with HDM/CSE for 24 h determined via ELISA. C IL--33 levels in mouse serum determined via ELISA. D Immunohistochemical staining of IL--33 in mouse lungs (scale bars, 100 μm) (n = 3). E Experimental schedule for the cigarette smoke--exposure asthma mouse model (with sST2 treatment). F R_L was determined in response to increasing methacholine (n = 3). G Histological examination of mouse lung sections stained with H&E (scale bars, 1 mm for 2x magnification and 100 μm for 20x magnification) and PAS (scale bars, 50 μm) (n = 3). H Diff--quick staining (scale bars, 50 μm) and cell counts of BALF (n = 4–5). I Eosinophils ($CD45^+CD11c^{low}CD11b^+SiglecF^+$) and neutrophils ($CD45^+CD11c^{low}CD11b^+Ly6G^+$) in the mouse lung and spleen (n = 3–4). J Matured DCs ($CD45^+CD11c^+CD40^+$ and $CD45^+CD11c^+CD86^+$) in the spleen were evaluated by flow cytometry (n = 3–4). K--M Th2 ($CD4^+$IL--4^+), Th17 ($CD4^+$IL--17 A^+), and Th1 ($CD4^+$IFN--γ^+) cells in the lung and spleen (n = 3–4). N Relative IL-4, IL-17A, and INF-γ mRNA levels in mouse spleen (n = 3) were determined by RT--qPCR. GAPDH was used as a loading control. The data are presented as the mean ± SEM. $^*P < 0.05$; $^{**}P < 0.01$.

groups, including 101 upregulated and 240 downregulated genes (Fig. 4A and Table S4). WGCNA was applied to identify gene modules highly involved in HDM/CS- and sST2-treated mice. A total of 4632 genes were classified into 8 modules based on gene expression data obtained via WGCNA (Fig. 4B and Fig. S7B-D-). We observed a unique gene module (brown module) that exhibited activation in the HDM/CS group and suppression in the HDM/CS/sST2 group, which may be implicated in the mechanism by which IL--33 participates in cigarette smoke--exposure asthma (Table S5). GO analyses of the 341 DEGs (Fig. 4C) and GO and KEGG analyses of the 1224 genes in the brown module (Fig. 4D and E) suggested that gene pathways related to eosinophil, monocyte, and neutrophil chemotaxis and migration; leukocyte migration; and T-cell differentiation are relevant to sST2 treatment. Importantly, we found that within pathways related to neutrophils, the NET formation pathway (KEGG: mmu04613) ranked first (Fig. 4D). In HDM/CS--treated mice, mTOR was downregulated, while Mpo, Fcgr1, Aqp9, Casp1, C3, Ncf1, Fcgr3, Cybb, and Clec7a were upregulated; all of these genes are known to be involved in NET formation; however, when mice were treated with sST2, all of these modulations were attenuated (Fig. 4F). These data suggest that IL--33 facilitates the granulocyte--associated response and is likely involved in NET formation.

3.3. NETs are abundantly produced and are correlated with poor lung function

We next evaluated NET formation in cigarette smoke--exposure asthma. In the BEAS--2B--neutrophil coculture condition, the levels of NET--associated Cit--H3, MPO--DNA, and HMGB1 were significantly increased in the HDM/CSE--treated group (Fig. 5A, B and Fig. S8). In addition, we observed a considerable amount of spontaneous NETs in HDM/CSE--treated neutrophils by fluorescence microscopy *in vitro* (Fig. 5C and D). *In vivo*, the Cit--H3 and MPO proteins were embedded in the extracellular DNA network structure of neutrophils (labelled with Ly6G) in the lungs of HDM/CS--treated mice (Fig. 5E and F) and the MPO--DNA levels were increased in the BALF of HDM/CS--treated mice compared with the control groups (Fig. 5G). As determined by ELISA, the serum levels of MPO--DNA and HMGB1 were markedly greater in asthma smokers than in healthy controls (Fig. 5H and I). Next, we assessed the correlations between NETs in the serum and FEV_1/predicted and FEV_1/FVC in asthma patients. FEV_1/predicted and FEV_1/FVC were negatively correlated with MPO-DNA and HMGB1 in the serum (Fig. 5J).

3.4. Molecular targets for NET formation are associated with DC--Th17 responses in vivo and in vitro

To better understand the role of NETs in asthma, we used the PAD inhibitor Cl--amidine to inhibit NET production and PMA as a positive control in some experiments in HDM/CS--treated mice (Fig. 6A and B). Cl--amidine--treated mice showed protection against HDM/CS--induced peribronchial inflammation and goblet cell hyperplasia, whereas PMA had the opposite effect (Fig. 6C). Inhibition of NETs also reduced the number of eosinophils and neutrophils in the BALF, lung, and spleen (Fig. 6D--G), the proportions of $CD40^+$ and $CD86^+$ splenic DCs (Fig. 6H), and the numbers of Th2 and Th17 cells in the lung and spleen (Fig. 6I--K).

To examine whether HDM/CSE-induced NETs could directly facilitate DC activation and Th2/Th17 cell generation, we collected human PBMCs to prepare DCs (Fig. S9 and Fig. 7A). Subsequently, the DCs were stimulated with HDM/CSE--induced NETs, while the controls were treated with HDM--induced NETs, IFN--γ, or PBS. In terms of antigen-specific T-cell responses, the harvested DCs were cocultured with naive $CD4^+$ T cells. We found that DCs stimulated with HDM/CSE-induced NETs expressed more CD40 and CD86 than unstimulated DCs (Fig. 7B and C) and promoted the increased production of Th2 and Th17 cells (Fig. 7D--H).

3.5. IL--33 induces NET formation in cigarette smoke--exposure asthma

We next explored the previously unexplored link between NETs and IL--33. *In vitro*, BEAS--2B cells were treated with 100 ng/mL recombinant human sST2 to inhibit the effect of IL--33 (Fig. S10). We found that IL--33 inhibition suppressed NETs in human neutrophil--BEAS--2B coculture conditions, as detected by immunostaining and western blotting (Fig. 8A--C). In contrast, with recombinant human IL-33, HDM/CSE-treated neutrophils were stimulated to produce more NETs (Fig. 8D-F). These results were further supported by *in vivo* analyses. Mice treated with sST2 displayed lower levels of Cit--H3 and colocalization of Cit--H3 with MPO in lung tissue (Fig. 8G and H). In addition, compared with HDM/CS-treated WT mice, HDM/CS--treated IL-33-KO mice presented attenuated expression of NET--related MPO-DNA and HMGB1 in the BALF and serum (Fig. 8I and J). They also showed decreased expression of eDNA in the BALF, as determined by PicoGreen (Fig. 8K), and less levels of NETs in lung (Fig. 8L). These findings suggested that the levels of NETs were regulated by the initiated inflammatory factor IL-33.

3.6. Autophagy is significantly increased in HDM/CS treated-neutrophils

Autophagy has also been reported to play an important role in the function of neutrophils.[38] In patients, we observed a trend toward increased expression of the LC3B and ATG5 genes and decreased expression of the p62 gene in neutrophils from asthma smokers (Fig. 9A). These results suggest that CS may elicit neutrophil autophagy in patients with asthma. Furthermore, we observed neutrophil autophagy in human neutrophil--BEAS--2B coculture conditions. We found an increase in the ratio of LC3B--II/LC3B--I and a decrease in p62 in the HDM/CSE--treated group (Fig. 9B). Since autophagy serves as a dynamic recycling system, we next analyzed autophagic flux. As shown in Fig. 9C, the increase in the LC3B--II protein in HDM/CSE--treated neutrophils was further enhanced after bafilomycin A1 administration, suggesting that the increase in LC3B--II was attributable to autophagy instead of impaired fusion of autophagosomes (APs) with lysosomes. These results were further confirmed by RT--qPCR (Fig. 9D--F). Consistently, in the lung tissues of HDM/CS--treated mice, we observed an increase in neutrophil autophagy, as visualized by colocalization of LC3B and the neutrophil marker Ly6G (Fig. 9G), as well as evident APs and autolysosomes (ALs) (Fig. 9H), compared with those in control mice.

3.7. Inhibition of autophagy ameliorates lung inflammation in mice

To further elucidate how autophagy regulates asthma-related inflammation, we used the autophagy inhibitor 3--MA and the

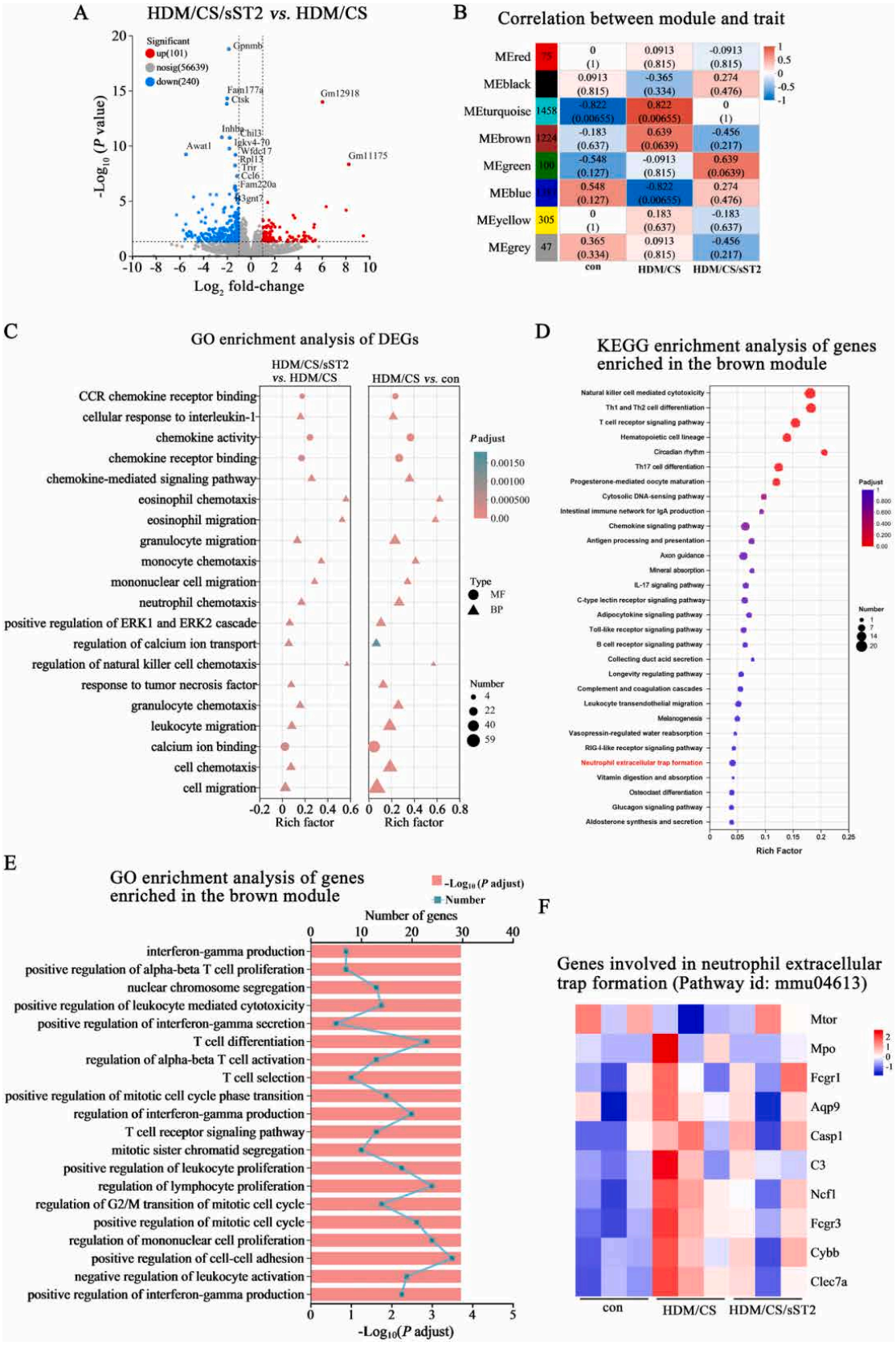

Fig. 4. IL--33 is associated with granulocyte, T cell, and NET formation–related gene pathways. A Volcano plot illustrating the analysis of DEGs between the HDM/CS/sST2 and HDM/CS groups. *P* value < 0.05 & $|\log_2$ (fold--change)$| > 1$. B Based on the gene expression data, 4632 genes were categorized into 8 modules using WGCNA. C Bubble chart of the multi--genome GO enrichment of DEGs. The top 20 enriched GO terms are listed (y-axis). The X-axis shows the enrichment factor. The bubble color represents the adjusted *P* value, and the bubble radius represents the gene number. D and E KEGG (D) and GO (E) enrichment analysis of genes enriched in the brown module (1224 genes). F Gene expression heatmap related to NET formation (pathway ID: mmuo4613).

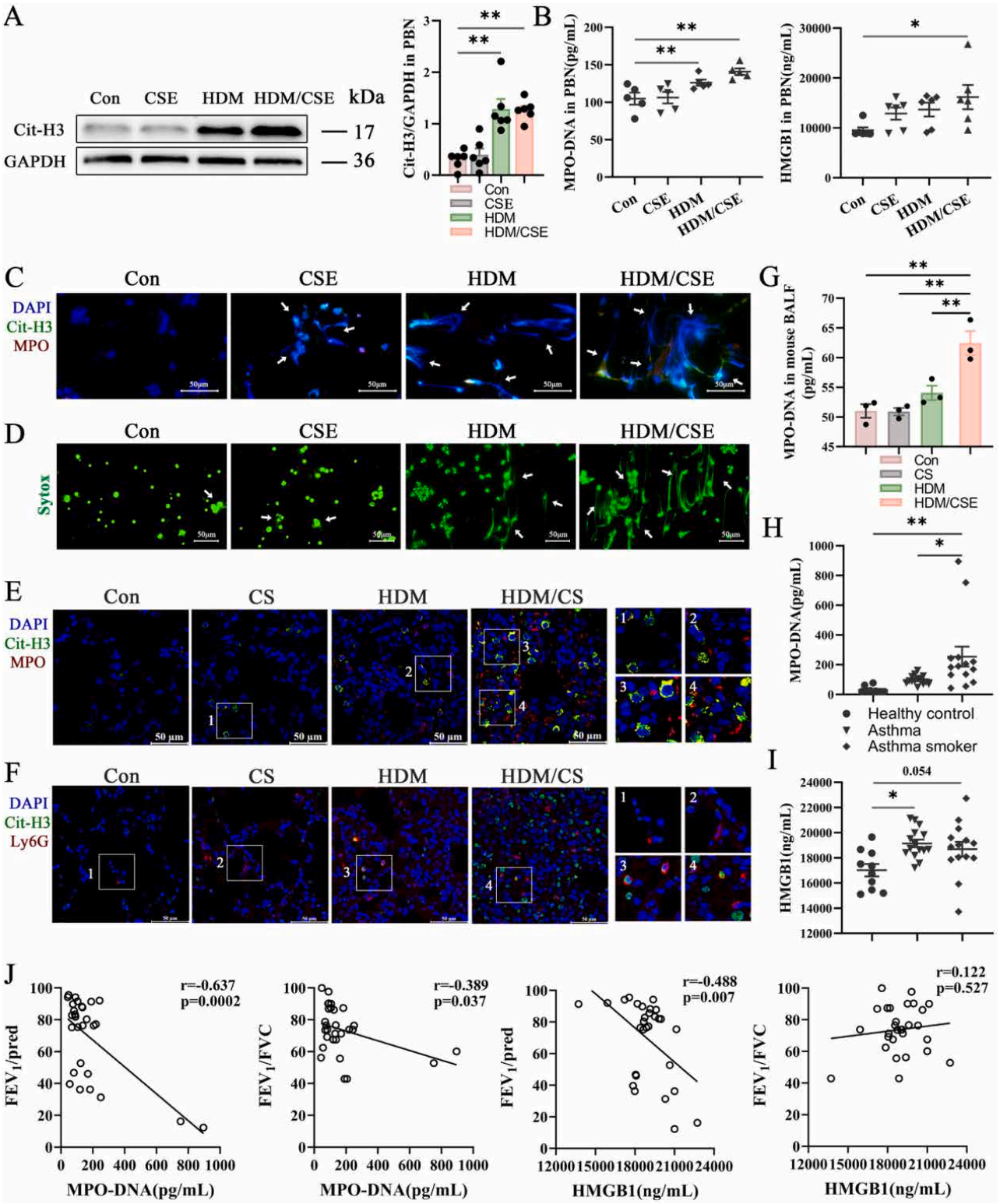

Fig. 5. NETs were increased and were correlated with poor lung function. A Representative immunoblots of Cit--H3 and GAPDH in human neutrophils from independent experiments (n = 6). B The levels of MPO-DNA and HMGB1 in neutrophil supernatants were measured via ELISA. C Immunofluorescence staining of Cit--H3 (green), MPO (red), and DAPI (blue) to visualize NET formation in human neutrophils (scale bars, 50 μm). NETs were indicated as Cit--H3/MPO double--positive cells shown by arrows. D Immunofluorescence images of SYTOX Green-stained neutrophils *in vitro* (scale bars, 50 μm). E Immunofluorescence staining of Cit--H3 (green), MPO (red) and DAPI (blue) in mouse lung sections visualized by confocal laser scanning microscopy (scale bars, 50 μm). Insets were magnified on the right side. F Immunofluorescence staining of Cit--H3 (green), Ly6G (red), and DAPI (blue) in mouse lung sections (scale bars, 50 μm). Insets were magnified on the right side. G MPO-DNA levels in BALF from mice determined by ELISA (n = 3). H and I Solute MPO--DNA (**H**) and HMGB1 (**I**) in serum from asthma smokers (n = 15), asthmatic patients (n = 14), and healthy controls (n = 10) determined by ELISA. **J** The correlations between MPO-DNA and HMGB1 in serum of asthma patients and FEV_1/predicted and FEV_1/FVC were determined via Pearson's correlation coefficient.

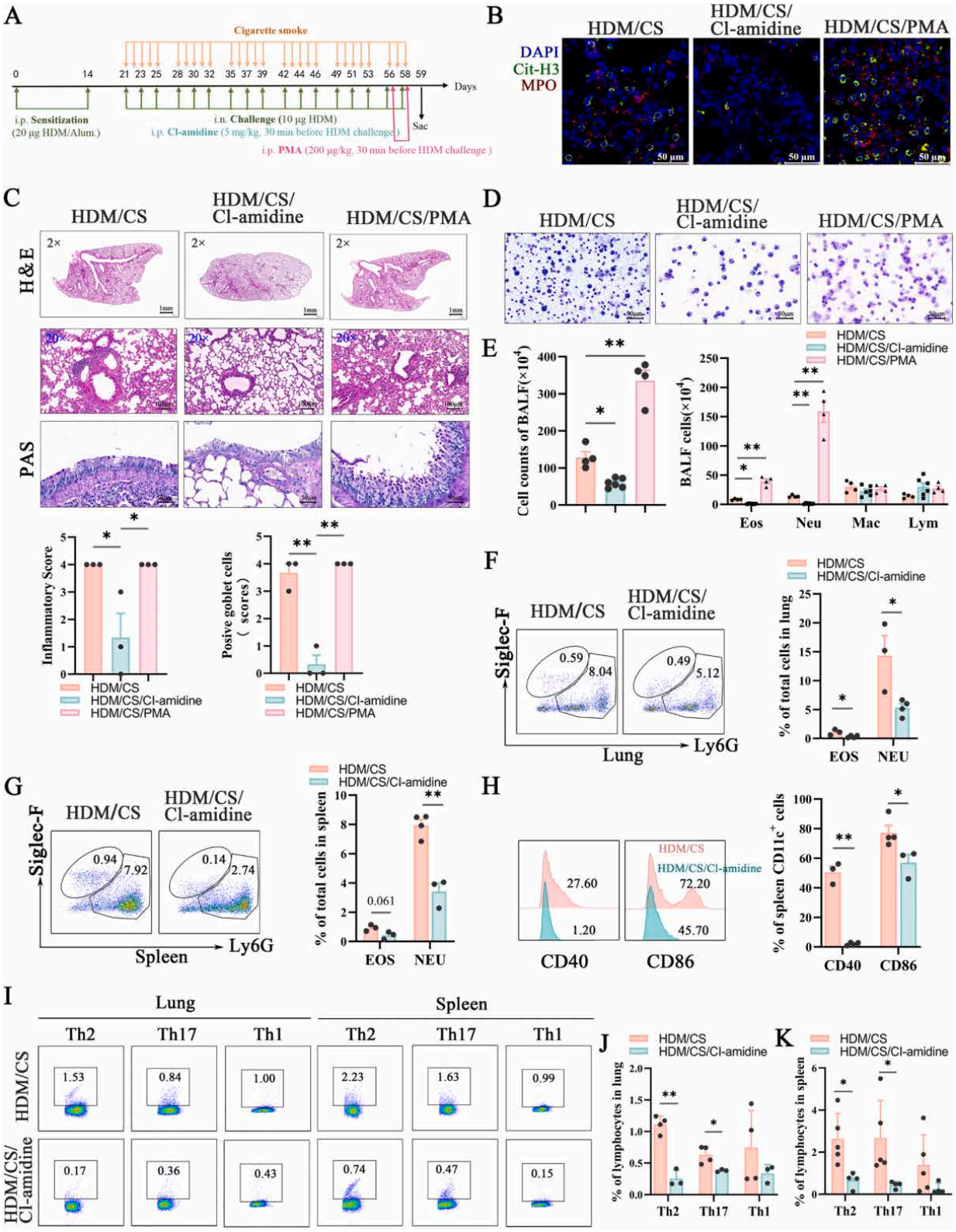

Fig. 6. NETs promote airway inflammation, DC activation, and Th2/Th17 responses *in vivo*. A Experimental timeline for the cigarette smoke--exposure asthma mouse model (with Cl--amidine or PMA treatment). B Representative immunofluorescence images of Cit-H3 (green) and MPO (red) in lung sections from mice were captured by confocal laser scanning microscopy (scale bars, 50 μm). C H&E (scale bars, 1 mm for 2x magnification and 100 μm for 20x magnification) and PAS (scale bars, 50 μm) staining of mouse lung sections (n = 3). D and E Diff--quick staining (scale bars, 50 μm) and cell counting of inflammatory cells in BALF (n = 4–6). F and G The proportions of eosinophils ($CD45^+CD11c^{low}CD11b^+SiglecF^+$) and neutrophils ($CD45^+CD11c^{low}CD11b^+Ly6G^+$) in the mouse lung (F) and spleen (G) (n = 3–4). H The proportions of mature DCs ($CD45^+CD11c^+CD40^+$ and $CD45^+CD11c^+CD86^+$ cells) in the spleen (n = 3–4). I--K The proportions of Th2 ($CD4^+IL\text{-}4^+$), Th17 ($CD4^+IL\text{-}17\ A^+$), and Th1 ($CD4^+IFN\text{-}\gamma^+$) cells in the lung and spleen were determined by flow cytometry (n = 3–5). The data are presented as the mean ± SEM. $^*P < 0.05$; $^{**}P < 0.01$.

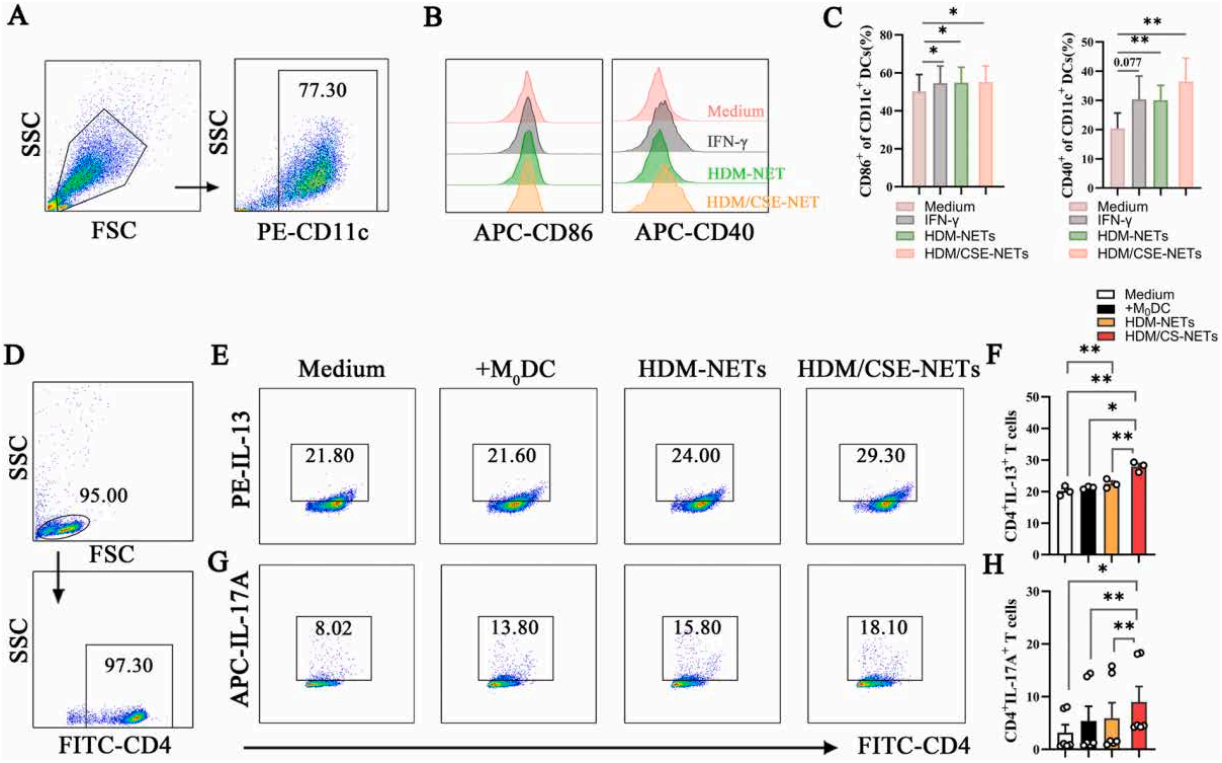

Fig. 7. HDM/CSE-induced NETs promote the activation of DCs, which facilitates the generation of Th2 and Th17 cells *in vitro.* A The purity of $CD11c^+$ cells identified as monocyte--derived DCs was detected by flow cytometry. B and C Expression of CD86 and CD40 on $CD11c^+$ DCs stimulated with PBS, IFN--γ, HDM--NETs, or HDM/CSE--NETs. D Purified naive $CD4^+$ T cells were isolated by negative selection and detected by flow cytometry. E--H Purified naive $CD4^+$ T cells were cocultured with DCs or PBS alone. Th2 (E and F) and Th17 (G and H) cells in the coculture condition were detected by flow cytometry. The data are presented as the mean ± SEM. $^*P < 0.05$; * $^*P < 0.01$.

autophagy agonist rapamycin *in vivo* following the protocol illustrated in Fig. 10A. When these HDM/CS--challenged mice were pretreated with 3--MA, the aggravated lung inflammation and mucus secretion were significantly reduced. However, after pretreatment with rapamycin, inflammation that occupied almost the entire lung was observed (Fig. 10B and C). Moreover, the inhibition of autophagy also markedly reduced the number of eosinophils and neutrophils in the BALF, lung, and spleen (Fig. 10D--G); the levels of CD40 and CD86 on splenic DCs (Fig. 10H); and the numbers of Th2 and Th17 cells in the lung and spleen (Fig. 10I--K).

3.8. *Feedforward connection between neutrophil autophagy and NET formation*

Recent studies have revealed cross--talk between NETs and autophagy.[39,40] Therefore, we wondered about the relationship between these two important neutrophil activities. In fact, we found that the increases in NET-related Cit--H3, HMGB1, MPO, and eDNA in neutrophils from asthma smokers were abolished by pretreatment with 3--MA and further enhanced by pretreatment with rapamycin (Fig. S11 and Fig. 11A--D). *In vivo,* 3--MA--pretreated mice had fewer Cit--H3 proteins and less colocalization of Cit--H3 with MPO in the lung than the mice treated with HDM/CS alone, whereas more NETs were visualized in rapamycin--pretreated mice (Fig. 11E and F). These data imply that neutrophil autophagy can modulate NET generation in cigarette smoke--exposure asthma.

In contrast, we examined whether NETs can mediate neutrophil autophagy by using the PAD inhibitor Cl--amidine and the NET inducer PMA. In comparison with those in HDM/CS--treated mice, Cl--amidine treatment resulted in reduced colocalization of LC3B with Ly6G and elevated p62 expression, while induction of NETs caused more neutrophils to undergo autophagy (Fig. 11G and H). Collectively, these data reveal a feedforward connection between HDM/CS--induced NETs and neutrophil autophagy.

Moreover, we investigated the regulatory effects of ROS on autophagy and NETs. Compared with those in the controls, the intracellular ROS in human neutrophils were increased in the HDM/CSE stimulation group (Fig. S12A). After treatment with N--Acetyl--L--cysteine (NAC), Cit--H3 and LC3B--II production were inhibited (Fig. S12B), indicating that both HDM/CSE--induced neutrophil autophagy and NETs are dependent on ROS production.

It is reported that autophagy influences NET formation through various pathways, including PI3K-AKT-mTOR, fMLP-FPR, Hif-1α-REDD1, Mincle signaling, and AMPK phosphorylation.[15–17,41–43] In ARDS models, NETs have been found to activate METTL3-mediated m6A methylation of Sirt1 mRNA, leading to autophagic dysfunction.[44] KEGG enrichment analysis identified potential involvement of PI3K/AKT/mTOR, AMPKα, and Hif-1α pathways in the autophagy-NET feedforward loop in HDM/CS-treated mice (Fig. 12A). To test this, we used a neutrophil-BEAS-2B co-culture system. Inhibiting PI3K (treated with 2 mM 3-MA for 4 h) led to decreased Hif-1α expression and increased p-mTOR, while mTOR inhibition (treated with 200 nM rapamycin for 4 h) increased Hif-1α levels compared to HDM/CSE treatment alone (Fig. 12B). In the co-culture, inhibiting NET formation (treated with 200 μM Cl-amidine for 15 min[45]) downregulated the HIF-1α pathway and upregulated p-mTOR, while stimulating NETs (treated with 100 nM PMA for 3 h[45]) had the opposite effect (Fig. 12C). This suggests the mTOR-Hif-1α pathway plays a key role in the autophagy-NET feedforward loop. Using 30 μM Hif-1α inhibitor (CAY10585) for 2 h in the co-culture reduced autophagy and NET formation, with no significant increase when combined with mTOR inhibition (Fig. 12D-G). These results support the central role of the mTOR-Hif-1α signaling pathway in the mutual regulation of autophagy and NET formation.

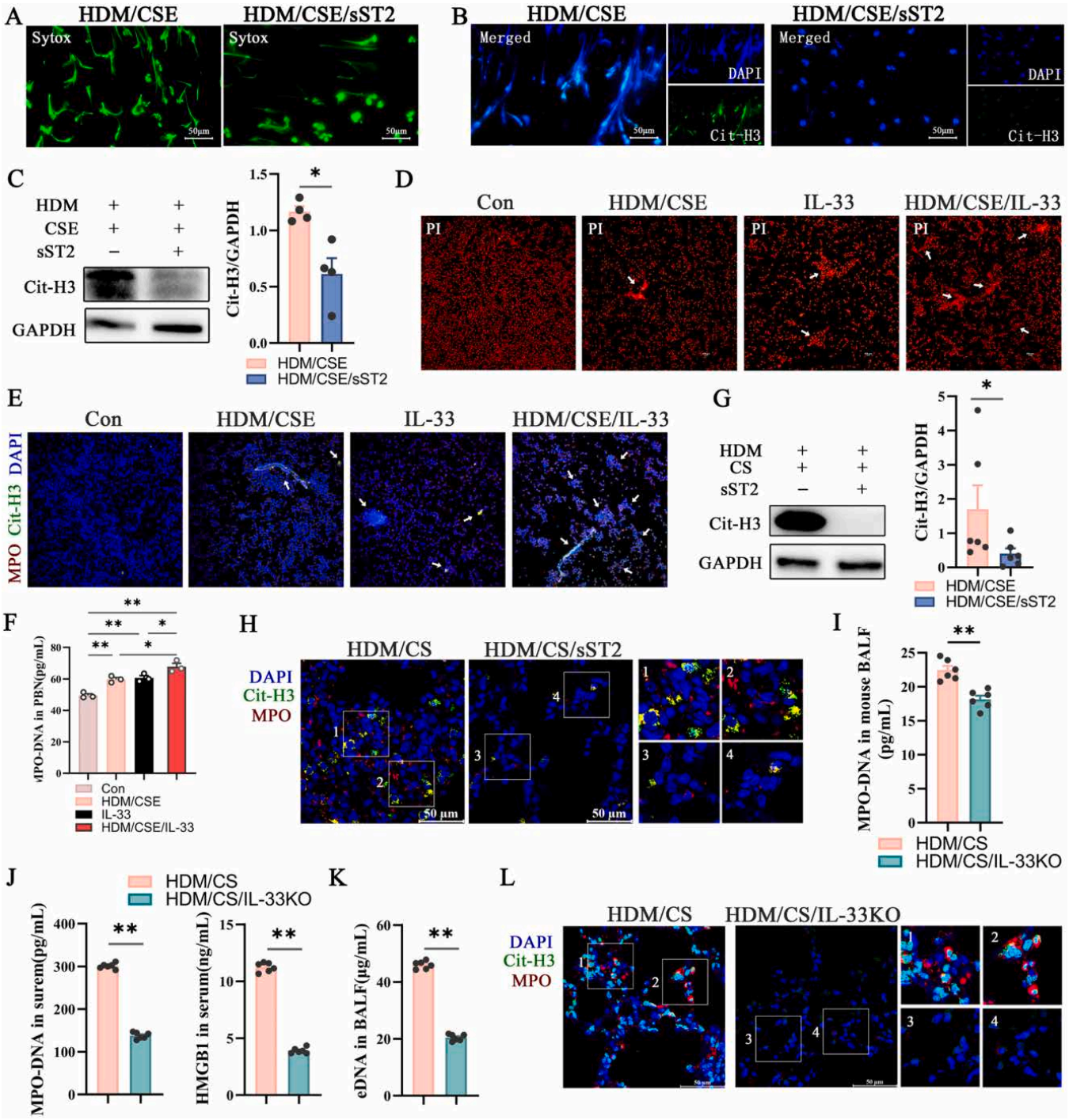

Fig. 8. IL--33 blockade suppresses NETs *in vitro* and *in vivo*. A SYTOX Green immunofluorescence staining of human neutrophils (scale bars, 50 μm). B Immunofluorescence staining of Cit--H3 (green) and DAPI (blue) were used to visualize NET formation in neutrophils *in vitro* (scale bars, 50 μm). C Cit-H3 in human neutrophils was detected via western blotting. D The dsDNA of neutrophils were stained with PI (scale bars, 100 μm). E Immunofluorescence staining of Cit--H3 (green) and MPO (red) were used to visualize NET formation in neutrophils (scale bars, 100 μm). F The levels of MPO--DNA in neutrophil supernatants were measured via ELISA. G Cit--H3 in the lung tissue of mice was detected via western blotting (n = 6). H Quantification of NETs in the lungs of mice by confocal laser scanning microscopy (Cit--H3, green; MPO, red; DAPI, blue) (scale bars, 50 μm). Insets were magnified on the right side. I Quantification of MPO--DNA levels in mouse BALF by ELISA (n = 6). J Quantification of MPO--DNA and HMGB1 levels in mouse serum by ELISA (n = 6). K The concentrations of extracellular DNA in the BALF of mice were investigated via a PicoGreen fluorescence quantitative assay (n = 6). L NETs in mouse lung were detected via immunofluorescence staining (Cit--H3, green; MPO, red; DAPI, blue) (scale bars, 50 μm). The data are presented as the mean ± SEM. *$P < 0.05$; * *$P < 0.01$.

3.9. IL--33 regulates mTOR--autophagy signaling to produce NETs in neutrophils

Finally, we speculated that IL--33 promotes NET formation through neutrophil autophagy. Under human neutrophil--BEAS--2B coculture conditions, we found that, compared with HDM/CSE alone, sST2 pretreatment decreased the LC3B--II protein and increased the p62 protein in neutrophils (Fig. 13A). At the transcriptional level, the LC3A, LC3B, and ATG5 genes were downregulated, while p62 and mTOR were upregulated in sST2--pretreated neutrophils (Fig. 13B). Recombinant

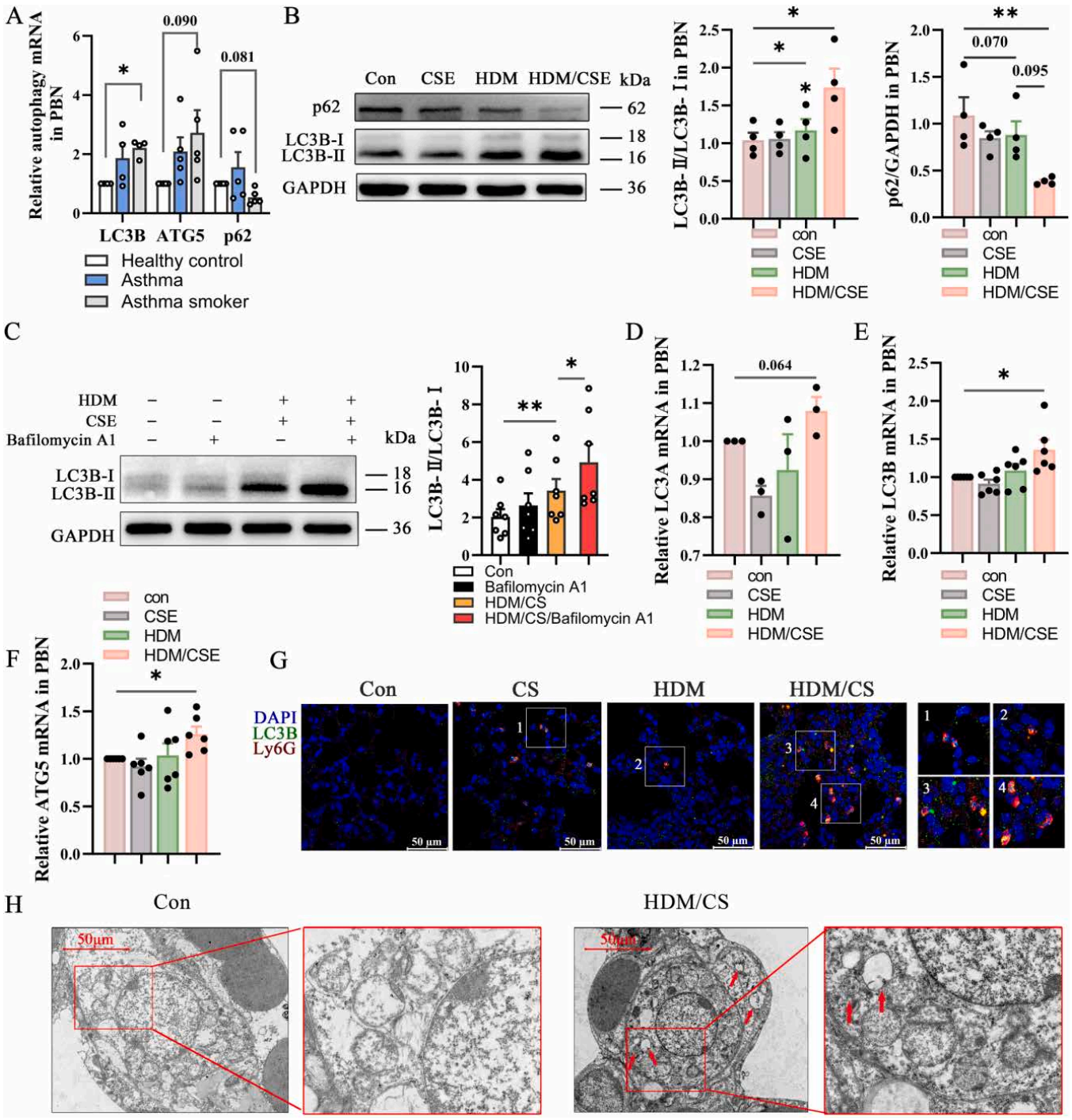

Fig. 9. Autophagy is significantly increased *in vitro* and *in vivo* in HDM/CS treated-neutrophils. A Relative LC3B, ATG5, and p62 mRNA levels in peripheral blood neutrophils from healthy controls, asthmatic patients, and asthmatic smokers (n = 4–5) were determined by RT--qPCR. GAPDH was used as a loading control. B Quantification of the protein levels of LC3B and p62 in human neutrophils by western blotting. C Detection of autophagic flux in human neutrophils after bafilomycin A1 stimulation. D-F Relative LC3A (D), LC3B (E), and ATG5 (F) mRNA levels in human neutrophils were determined by RT--qPCR. GAPDH was used as a loading control. G Quantification of neutrophil autophagy in mouse lung sections by confocal laser scanning microscopy (LC3B, green; Ly6G, red; DAPI, blue) (scale bars, 50 μm). Insets were magnified on the right side. H Representative images of APs and ALs (red arrows) in mouse lung sections observed via transmission electron microscopy (scale bars, 50 μm). The data are presented as the mean ± SEM. *$P < 0.05$; * *$P < 0.01$.

human IL-33 induced more colocalization of LC3B and LAMP-1 in neutrophils from healthy donors, especially with concurrent treatment with HDM/CSE (Fig. 13C). Similar observations were noted in the lung tissues of ST2-pretreated mice by immunofluorescence double staining and western blotting (Fig. 13D and E). Furthermore, the number of APs and ALs in the lungs of HDM/CS--treated IL--33KO mice was almost abolished compared with that in the lungs of HDM/CS--treated WT mice (Fig. 13F). Hence, these data support the notion that the inhibition of IL--33 suppresses HDM/CS--induced neutrophil autophagy. To further validate our hypothesis, under human neutrophil--BEAS--2B coculture conditions, we administered sST2 in combination with the mTOR inhibitor rapamycin. We found that changes in Cit--H3 and p62 expression induced by sST2 were reversed after rapamycin treatment (Fig. 13G). These results provide proof that IL--33 augments mTOR-related

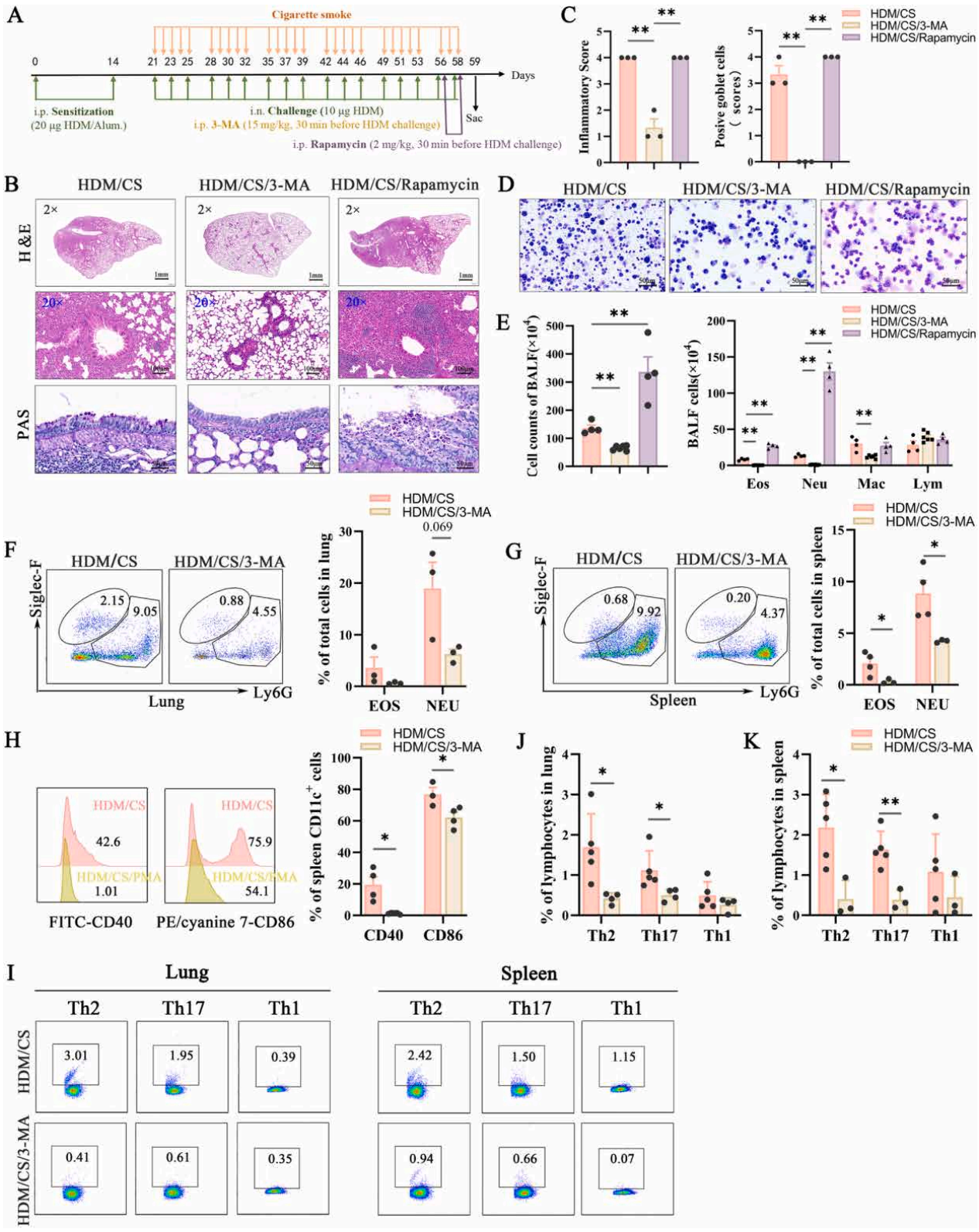

Fig. 10. Autophagy is related to neutrophilic airway inflammation and DC--Th17 responses in mice. A Experimental timeline for the cigarette smoke-exposure-induced asthma mouse model (with 3--MA or rapamycin treatment). B and C Representative images of mouse lung sections stained with H&E (scale bars, 1 mm for 2x magnification and 100 μm for 20x magnification) and PAS (scale bars, 50 μm) (n = 3). D and E Diff--quick staining (scale bars, 50 μm) and inflammatory cell counts in the BALF (n = 4–6). F and G The ratio of eosinophils ($CD45^{+}CD11c^{low}CD11b^{+}SiglecF^{+}$) and neutrophils ($CD45^{+}CD11c^{low}CD11b^{+}Ly6G^{+}$) in the mouse lung (F) and spleen (G) was determined by flow cytometry (n = 3–4). H The ratio of mature DCs ($CD45^{+}CD11c^{+}CD40^{+}$ and $CD45^{+}CD11c^{+}CD86^{+}$ cells) in the spleen (n = 3–4). I--K The ratio of Th2 ($CD4^{+}IL\text{--}4^{+}$), Th17 ($CD4^{+}IL\text{--}17\ A^{+}$), and Th1 ($CD4^{+}IFN\text{--}\gamma^{+}$) cells in the lung and spleen determined by flow cytometry (n = 3–5). The data are presented as the mean ± SEM. $^{*}P < 0.05$; $^{**}P < 0.01$.

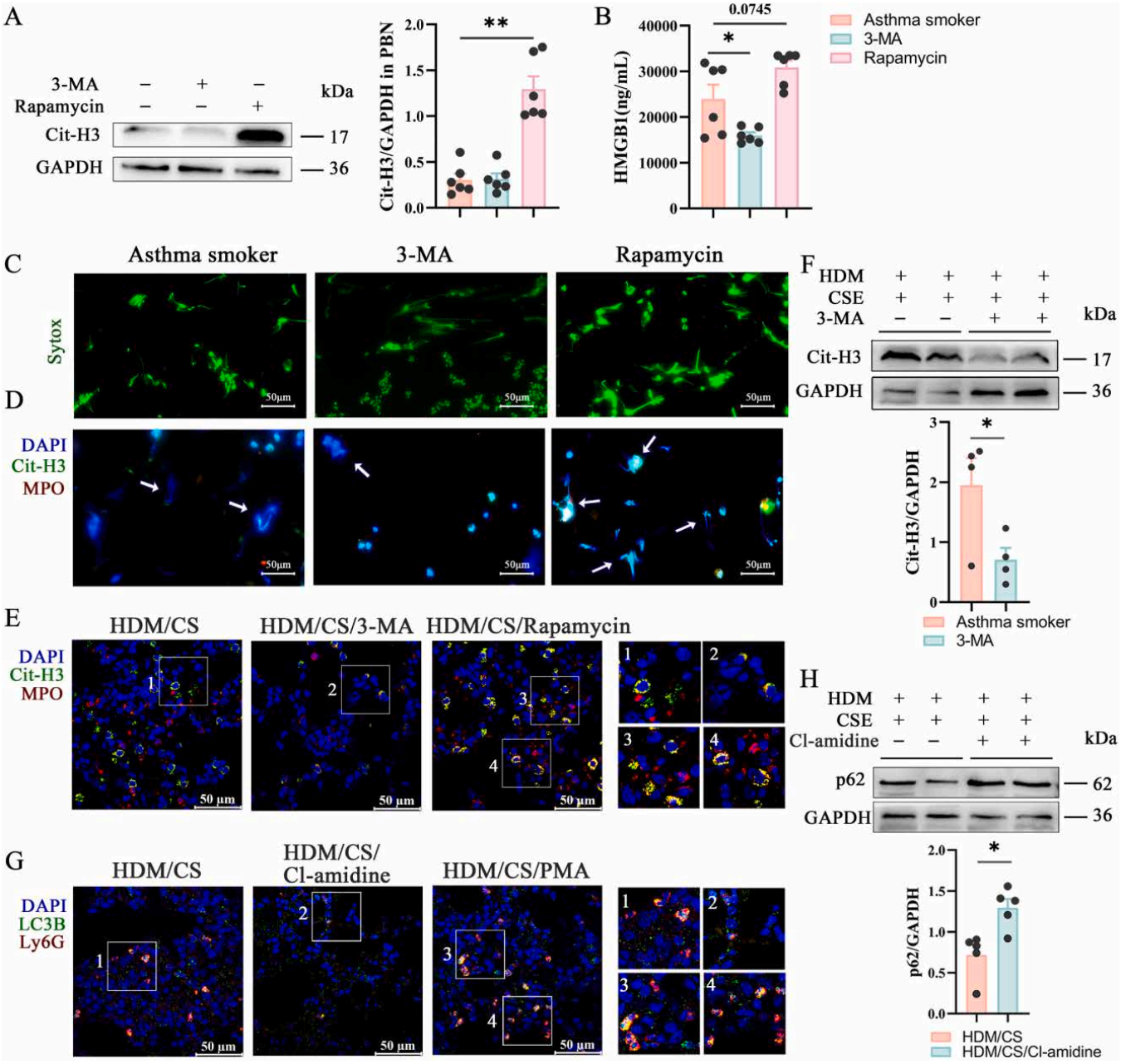

Fig. 11. Neutrophil autophagy augments NET production, and autophagy formation depends on NETs. A Representative immunoblots of Cit--H3 and GAPDH in peripheral blood neutrophils from asthma smokers. B Concentrations of HMGB1 in neutrophil supernatants from asthma smokers determined via ELISA. C Representative immunofluorescence images of neutrophils from asthma smokers stained with SYTOX Green (scale bars, 50 μm). D Quantification of NETs in neutrophils from asthma smokers by Cit--H3 (green), MPO (red), and DAPI (blue) staining (scale bars, 50 μm). E Cit--H3 (green), MPO (red), and DAPI (blue) staining of mouse lung sections was performed via confocal laser scanning microscopy (scale bar, 50 μm). Insets are magnified on the right side. F Representative immunoblots of Cit--H3 protein in mouse lung tissue. G Neutrophil autophagy (LC3B, green; Ly6G, red; DAPI, blue) in mouse lungs was assessed by confocal laser scanning microscopy (scale bar, 50 μm). Insets were magnified on the right side. H Representative immunoblots of the p62 protein in mouse lung tissue. The data are presented as the mean ± SEM. *$P < 0.05$; * *$P < 0.01$.

autophagy in neutrophils, which in turn induces NET production.

4. Discussion

In the present study, we demonstrated that IL-33 regulated neutrophil activation is a critical mechanism of adaptive immunity in cigarette smoke--exposure asthma. A neutrophil--related phenotype underlies cigarette smoke--exposure asthma. Disruption of IL-33 inhibits the DC-Th2/Th17 immune response, mixed granulocytic inflammation, and AHR, by suppressing neutrophil -autophagy-mTOR-Hif-1α--NET formation. Our data revealed that neutrophil autophagy and NETs provide possible biomarkers for refractory neutrophilic asthma, and that targeting IL-33 and neutrophil function plays a major role in the treatment.

The immunopathophysiology of asthma involves interplay between epithelia and both innate and adaptive immune cells, along with challenge by CS, allergens, pathogens, and other exogenous substances.[46, 47] Understanding the different endotypes of asthma can help to provide individualized and targeted treatment for asthmatic patients. A high cumulative CS exposure is related to T2--low asthma, and

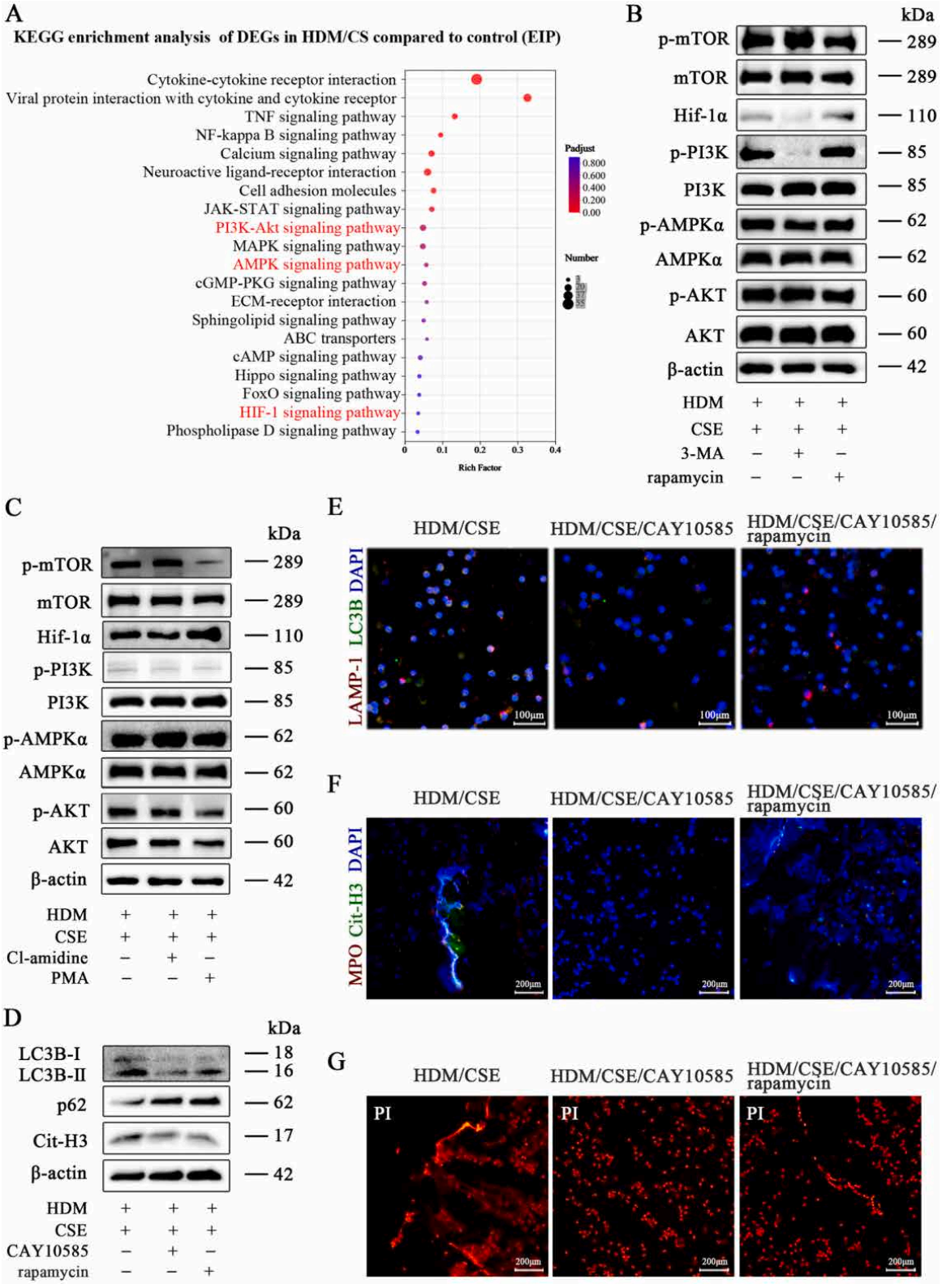

Fig. 12. Neutrophils form a feedforward loop of NETs-mTOR-Hif-α autophagy. A KEGG pathway analysis of DEGs (EIP). The top 20 enriched biological functions are presented on the basis of the *P* value (y-axis). The x-axis indicates the -$\log_{10}$ adjusted *P* value. The number represents the number of genes. B and C Immunoblot analysis of the indicated phosphorylated and total protein in PI3K/AKT/mTOR, AMPKα, and Hif-1α pathways of human neutrophils. D LC3B, p62, and Cit-H3 protein of human neutrophils stimulated with CAY10585 or rapamycin was detected via western blotting. E Representative immunofluorescence images of autophagy in neutrophils (LC3B, green; LAMP-1, red; DAPI, blue). (scale bars, 200 μm). F Immunofluorescence staining of Cit--H3 (green) and MPO (red) were used to visualize NET formation in neutrophils (scale bars, 200 μm). G The dsDNA of neutrophils were stained with PI (scale bars, 200 μm).

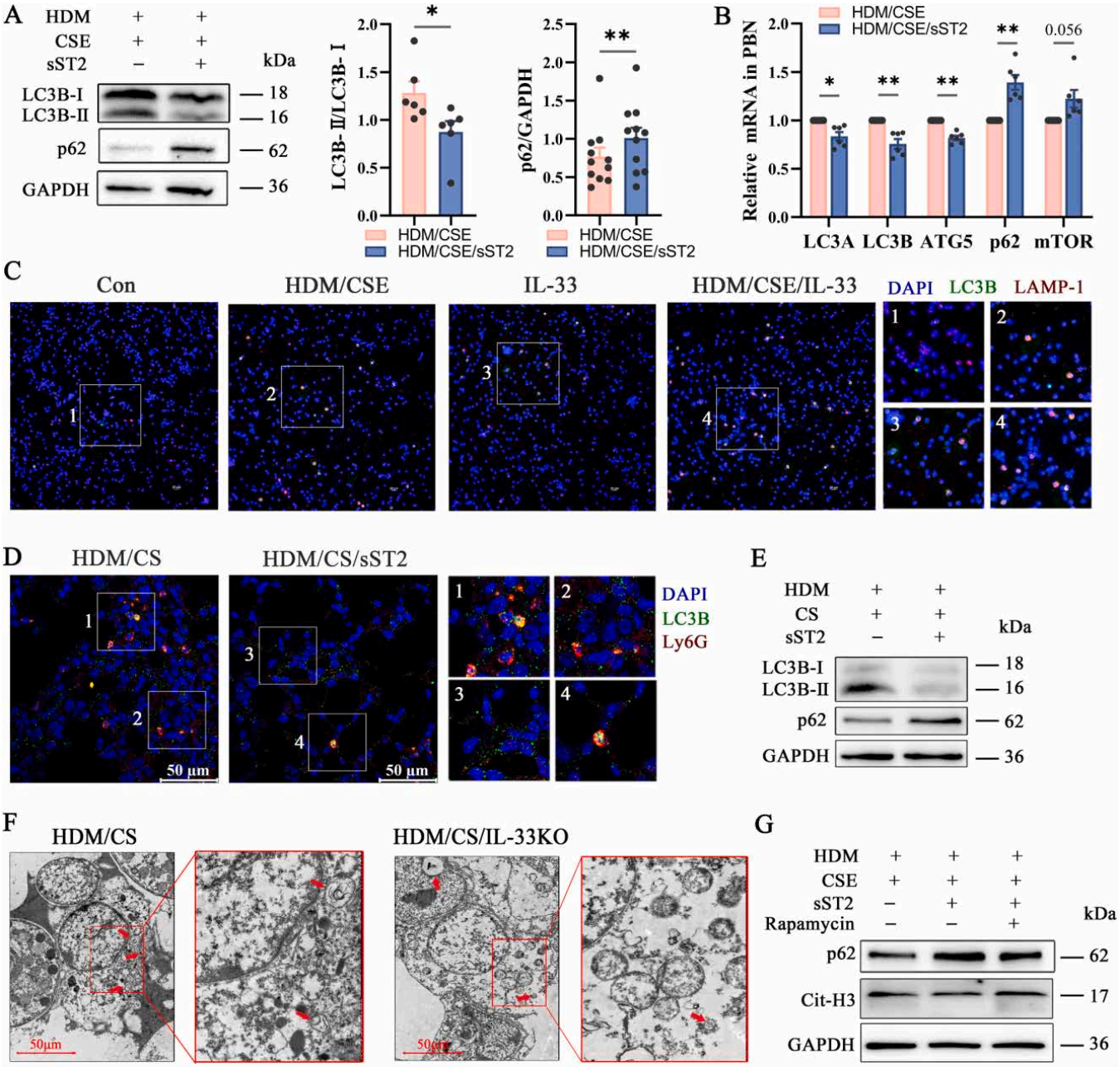

Fig. 13. Antagonizing IL--33 inhibits neutrophil mTOR- autophagy and thus NETs. A Representative immunoblots of the LC3B and p62 protein in human neutrophils. B Relative LC3A, LC3B, ATG5, p62, and mTOR mRNA levels in human neutrophils determined by RT--qPCR. GAPDH was used as a loading control. C Representative immunofluorescence images of autophagy in neutrophils (LC3B, green; LAMP-1, red; DAPI, blue). (scale bars, 20 μm). D Quantification of neutrophil autophagy in the lungs of mice by confocal laser scanning microscopy (LC3B, green; Ly6G, red; DAPI, blue). (scale bars, 50 μm). E Representative immunoblots of the LC3B and p62 proteins in mouse lungs. F Representative images of APs and ALs (red arrows) in mouse lungs viewed via transmission electron microscopy (scale bars, 50 μm). G Representative immunoblots of Cit--H3 and p62 in human neutrophils. The data are presented as the mean ± SEM. *$P < 0.05$; * *$P < 0.01$.

approximately 50 % of adults with asthma and a smoking history have neutrophilic or granulocytic airway inflammation.[48,49] Increased total IgE associated with active smoking may occur even in patients with asthma.[50,51] The CSE also regulates DC--mediated immune responses by influencing both DC function and maturation.[52] In agreement with this, our results demonstrated that, compared with HDM--induced eosinophilic allergic asthma, asthmatic mice exposed to CS results in neutrophilic airway inflammation, greater goblet cell hyperplasia, and airway remodeling, as well as more mature DCs and Th2 and Th17 cell counts. However, the development of validated treatments for neutrophilic inflammation is still a major challenge.

Exposure to CS or oxidative stress damages epithelia, leading to the release of IL--33.[53] The receptor ST2 for IL--33 is expressed on various immune cells, including eosinophils, macrophages, basophils, and $CD4^+$ T cells. The binding of IL--33 to ST2 promotes inflammation and serves as a central mediator in both innate and adaptive immune responses.[53] The deletion of IL--33 was found to affect the infusion of eosinophils, neutrophils and $ST2^+CD4^+$ T cells in chronic HDM--induced airway inflammation.[54] Nevertheless, the effects of IL--33 on neutrophil functions are poorly understood compared with those of eosinophils in asthma. It is debated whether neutrophils express ST2.[55] Our data showed that CS enhances the release of IL--33, which facilitates neutrophilic-- and eosinophilic--associated inflammation and Th2/Th17 responses. We provide evidence that IL-33 modulation of

neutrophil activation has a critical impact on the development of cigarette smoke--exposure asthma.

Activated neutrophils produce ROS, proteases, inflammatory agents, and can form NETs.[8] Previous studies show that NETs have been found to enhance antigen presentation by DCs, thereby augmenting the Th2 response in LPS- and HDM--induced asthma.[55] However, its role in airway immunopathology of cigarette smoke--exposed patients with asthma remains unknown. Here we observed that the increased NETs in lung and blood samples are associated with the poor lung function, inflammatory cell infiltration, and goblet cell hyperplasia in cigarette smoke--exposure asthma. Furthermore, NET stimulation drove DC activation, and naive $CD4^+$ T cells were exposed to allergens, which resulted in Th2/Th17 differentiation. Therefore, our study extends the current understanding of NETs in cigarette smoke--exposure asthma, suggesting that NETs may be a novel therapeutic target.

Autophagy in neutrophils is also involved in various functions, including phagocytosis, cytokine production, and degranulation, all of which are crucial for inflammation and defense against pathogens.[56] CS--exposed neutrophils exhibit increased autophagy, and their ability to ingest respiratory pathogens is compromised, which may promote further recruitment of neutrophils to the lung.[57] Here, our findings indicate that CS exposure increases neutrophil autophagy to aggravate granulocytic lung inflammation and the DC--Th2/Th17 immune response in asthma. Yet, the underlying mechanism has remained unclear. It has been reported that activation of autophagy is associated with the production of NETs to increase asthma severity.[58] The PI3K--AKT--mTOR pathway links autophagy and NETs.[15,41] In addition, studies have identified other molecular mechanisms involved in autophagy-dependent NETs, such as fMLP-FPR pathway,[16] Hif-1α-REDD1,[42] Mincle signaling,[17] and AMPK phosphorylation.[43] NETs activated METTL3 mediated-m6A methylation of Sirt1 mRNA in alveolar epithelial cells, resulting in abnormal autophagy.[44] Intracellular ROS levels determine whether autophagy activity ends in NETosis.[59,60] Alternatively, when invaded by pathogens, activated neutrophils produce effector molecules such as ROS, proteinases, and NETs, all of which can activate neutrophil autophagy.[61] Here our data demonstrate that autophagy agonist rapamycin induced NET release by inhibiting mTOR, whereas the inhibition of autophagy via 3--MA, a PI3K inhibitor, reduced NET formation. In turn, NET formation is dependent on neutrophil autophagy, and there is a feedforward loop between NETs and neutrophil autophagy. Notably, both autophagy and NET production are dependent on ROS, and the mTOR-Hif-1α signaling pathway is involved in the mutual regulation of autophagy and NET formation. Collectively, these data suggest that the important role of NETs in exacerbating cigarette smoke--exposure asthma is inextricably linked to neutrophil autophagy activity and the mTOR-Hif-1α signaling pathway.

We further investigated the effects of IL--33 on neutrophil functions. Several studies have shown that in mouse model of liver injury and rhinovirus-infected asthma, IL--33 promotes neutrophil recruitment and downstream NETosis.[62,63] On the basis of our findings, we found that blockade of IL--33 by sST2 reduces neutrophil autophagy to form NETs and that this effect can be reversed by the mTOR inhibitor rapamycin. These results indicate that human peripheral blood neutrophils and mouse lung tissues express ST2 and that IL--33/ST2 signaling contributes to the pathophysiologic role of cigarette smoke--exposure asthma by targeting neutrophils. However, to our knowledge, little is known about the effect of IL--33 on autophagy in asthma, and our study provides the first evidence that IL--33 induces neutrophil autophagy in asthma-related inflammation. Nevertheless, IL--33 was found to engage in autophagy in other cell types. In allergic rhinitis, IL--33 has been reported to stimulate degranulation of mast cells by inhibiting ST2/PI3K/mTOR--mediated autophagy.[64] A recent study has shown that neutrophils are heterogeneous and plastic and capable of adapting context--specific cues to fulfill particular functions.[65] Neutrophils exhibit different patterns of gene expression in accordance with their developmental stage and microenvironment.[66] Additionally, it is postulated that ST2 is expressed on a low proportion of neutrophils and that IL--33- induced autophagy and NETosis is a condition--specific phenomenon.[63] Although our study did not reveal the molecular pathways involved in IL-33--induced neutrophil activation, nor did it fully explore the mechanisms driving the feedforward loop between NET formation and autophagy *in vivo*, follow--up studies will delve deeper into these aspects to identify novel targets for effectively managing cigarette smoke-exposure asthma.

5. Conclusions

In conclusion, we demonstrated that epithelium--derived IL--33 drives the mixed granulocytic airway immune response in cigarette smoke--exposure asthma by interacting with neutrophil-autophagy-mTOR-Hif-1α driving NET formation. Our study established a previously unappreciated IL--33--autophagy--NET axis in asthma patients who responded to CS and identified it as a potential therapeutic strategy.

Environmental implication

Cigarette smoke is one of the most extensively studied environmental risk factors for respiratory diseases, affecting nearly all organ systems through mechanisms such as inflammation and DNA damage. Exposure to cigarette smoke is associated with increased risk of asthma incidence, poor clinical control, decreased lung function, and poor response to corticosteroids. Our study indicates that IL-33 stimulates the activation of the neutrophil autophagy-NET pathway, intensifying both Th2/Th17 responses and neutrophilic inflammation in cigarette smoke-exposure asthma. These findings might offer potential avenues for developing therapeutic strategies to alleviate exacerbations in asthma patients exposed to cigarette smoke.

Ethical approval

The clinical study was approved by the Ethics Committee of the Third Affiliated Hospital of Sun Yat--sen University (No. RG2023–271–02). All mice procedures were supported by the Institutional Animal Care and Use Committee of Jennio Biotech Co., Ltd. (No. JENNIO--IACUC--2023-A015). The certificates of approval are available upon request.

Funding

This study was funded by grants from National Natural Science Foundation of China (No. 82370034 and 81973984) and Guangzhou Municipal Science and Technology Project (No. 2024A03J0173).

Author statement

Jing Liu, **Peizhi Tao**, and **Beiting Su** designed the study, performed the clinical and mice experiments, contributed to acquisition of data, and wrote the manuscript. **Li Zheng** and **Yusen Lin** helped with the *in vitro* experiments from clinical samples. **Xiaoling Zou** and **Hailing Yang** helped with mice experiments and data analysis. **Wenbin Wu** provided advice about RNA--seq analysis and interpreted the data. **Hongtao Li** and **Tiantuo Zhang** conceived and initiated this study, guided and supervised the progress of experiments, interpreted the data, and revised the manuscript. All authors have read and approved the final manuscript.

CRediT authorship contribution statement

Jing Liu: Writing – original draft, Methodology, Investigation, Formal analysis, Data curation. **Hongtao Li:** Writing – review & editing, Visualization, Validation, Supervision, Project administration, Funding acquisition, Conceptualization. **Tiantuo Zhang:** Writing – review &

editing, Visualization, Validation, Supervision, Project administration, Conceptualization. **Wenbin Wu:** Methodology, Formal analysis. **Hailing Yang:** Methodology, Formal analysis. **Xiaoling Zou:** Methodology, Formal analysis. **Yusen Lin:** Methodology, Formal analysis, Data curation. **Li Zheng:** Methodology, Formal analysis, Data curation. **Beiting Su:** Writing – original draft, Methodology, Investigation, Formal analysis, Data curation. **Peizhi Tao:** Writing – original draft, Methodology, Investigation, Formal analysis, Data curation.

Declaration of Competing Interest

The authors declare that they have no known competing financial interests or personal relationships that could have appeared to influence the work reported in this paper.

Acknowledgements

We thank all of the patients and healthy controls who participated in this study. We gratefully thank Prof. Kefang Lai and Dr. Chuqin Huang (State Key Laboratory of Respiratory Disease, the First Affiliated Hospital of Guangzhou Medical University, Guangzhou, China.) for the technical supports of lung function assessment in mice. The current manuscript was revised by a native English speaking editor at American Journal Experts (AJE).

Appendix A. Supporting information

Supplementary data associated with this article can be found in the online version at doi:10.1016/j.jhazmat.2025.137257.

Data Availability

Data will be made available on request.

References

[1] Russell, R.J., Boulet, L.P., Brightling, C.E., Pavord, I.D., Porsbjerg, C., Dorscheid, D., et al., 2024. The airway epithelium: an orchestrator of inflammation, a key structural barrier and a therapeutic target in severe asthma. Eur Respir J 64, 2301397.
[2] Boulet, L.P., Lemière, C., Archambault, F., Carrier, G., Descary, M.C., Deschesnes, F., 2006. Smoking and asthma: clinical and radiologic features, lung function, and airway inflammation. Chest 129, 661–668.
[3] Wu, D., Lai, T., Yuan, Y., Chen, M., Xia, J., Li, W., et al., 2017. Elevated expression of placental growth factor is associated with airway-wall vascular remodelling and thickening in smokers with asthma. Sci Rep 7, 43017.
[4] Takahashi, K., Pavlidis, S., Ng Kee Kwong, F., Hoda, U., Rossios, C., Sun, K., et al., 2018. Sputum proteomics and airway cell transcripts of current and ex-smokers with severe asthma in U-BIOPRED: an exploratory analysis. Eur Respir J 51, 1702173.
[5] White, P.C., Hirschfeld, J., Milward, M.R., Cooper, P.R., Wright, H.J., Matthews, J. B., et al., 2018. Cigarette smoke modifies neutrophil chemotaxis, neutrophil extracellular trap formation and inflammatory response-related gene expression. J Periodontal Res 53, 525–535.
[6] Ham, J., Kim, J., Sohn, K.H., Park, I.W., Choi, B.W., Chung, D.H., et al., 2022. Cigarette smoke aggravates asthma by inducing memory-like type 3 innate lymphoid cells. Nat Commun 13, 3852.
[7] Ravensberg, A.J., Slats, A.M., van Wetering, S., Janssen, K., van Wijngaarden, S., de Jeu, R., et al., 2013. CD8(+) T cells characterize early smoking-related airway pathology in patients with asthma. Respir Med 107, 959–966.
[8] Thomson, N.C., Polosa, R., Sin, D.D., 2022. Cigarette Smoking and Asthma. J Allergy Clin Immunol Pr 10, 2783–2797.
[9] Thomson, N.C., 2017. Asthma and smoking-induced airway disease without spirometric COPD. Eur Respir J 49, 1602061.
[10] Polosa, R., Russo, C., Caponnetto, P., Bertino, G., Sarvà, M., Antic, T., et al., 2011. Greater severity of new onset asthma in allergic subjects who smoke: a 10-year longitudinal study. Respir Res 12, 16.
[11] Almyroudis, N.G., Grimm, M.J., Davidson, B.A., Röhm, M., Urban, C.F., Segal, B.H., 2013. NETosis and NADPH oxidase: at the intersection of host defense, inflammation, and injury. Front Immunol 4, 45.
[12] Jorch, S.K., Kubes, P., 2017. An emerging role for neutrophil extracellular traps in noninfectious disease. Nat Med 23, 279–287.
[13] Dworski, R., Simon, H.U., Hoskins, A., Yousefi, S., 2011. Eosinophil and neutrophil extracellular DNA traps in human allergic asthmatic airways. J Allergy Clin Immunol 127, 1260–1266.
[14] Lachowicz-Scroggins, M.E., Dunican, E.M., Charbit, A.R., Raymond, W., Looney, M.R., Peters, M.C., et al., 2019. Extracellular DNA, Neutrophil Extracellular Traps, and Inflammasome Activation in Severe Asthma. Am J Respir Crit Care Med 199, 1076–1085.
[15] Yu, Y., Sun, B., 2020. Autophagy-mediated regulation of neutrophils and clinical applications. Burns Trauma 8 tkz001.
[16] Itakura, A., McCarty, O.J., 2013. Pivotal role for the mTOR pathway in the formation of neutrophil extracellular traps via regulation of autophagy. Am J Physiol Cell Physiol 305, C348–354.
[17] Sharma, A., Simonson, T.J., Jondle, C.N., Mishra, B.B., Sharma, J., 2017. Mincle-mediated neutrophil extracellular trap formation by regulation of autophagy. J Infect Dis 215, 1040–1048.
[18] Marone, G., Spadaro, G., Braile, M., Poto, R., Criscuolo, G., Pahima, H., et al., 2019. Tezepelumab: a novel biological therapy for the treatment of severe uncontrolled asthma. Expert Opin Invest Drugs 28, 931–940.
[19] Bel, E.H., Ten Brinke, A., 2017. New Anti-Eosinophil Drugs for Asthma and COPD: Targeting the Trait! Chest 152, 1276–1282.
[20] Liu, J., Su, B.T., Tao, P.Z., Yang, X.N., Zheng, L., Lin, Y.S., et al., 2024. Interplay of IL-33 and IL-35 Modulates Th2/Th17 Responses in Cigarette Smoke Exposure HDM-Induced Asthma. Inflammation 47, 173–190.
[21] Yang, X.N., Su, B.T., Liu, J., Zheng, L., Tao, P.Z., Lin, Y.S., et al., 2023. A CpG-Oligodeoxynucleotide Suppresses Th2/Th17 inflammation by inhibiting IL-33/ST2 signaling in mice from a model of adoptive dendritic cell transfer of smoke-induced asthma. Int J Mol Sci 24, 3130.
[22] Jin, R., Xu, J., Gao, Q., Mao, X., Yin, J., Lu, K., et al., 2020. IL-33-induced neutrophil extracellular traps degrade fibronectin in a murine model of bronchopulmonary dysplasia. Cell Death Discov 6, 33.
[23] Wang, X., Li, X., Chen, L., Yuan, B., Liu, T., Dong, Q., et al., 2020. Interleukin-33 facilitates cutaneous defense against Staphylococcus aureus by promoting the development of neutrophil extracellular trap. Int Immunopharmacol 81, 106256.
[24] Quoc, Q.L., Cao, T.B.T., Jang, J.H., Shin, Y.S., Choi, Y., Park, H.S., 2024. ST2-Mediated Neutrophilic Airway Inflammation: A Therapeutic Target for Patients With Uncontrolled Asthma. Allergy Asthma Immunol Res 16, 22–41.
[25] Stojkov, D., Yousefi, S., Simon, H.U., 2024. NETs: Important players in asthma? J Allergy Clin Immunol 153, 100–102.
[26] Tan, Y.Y., Zhou, H.Q., Lin, Y.J., Yi, L.T., Chen, Z.G., Cao, Q.D., et al., 2022. FGF2 is overexpressed in asthma and promotes airway inflammation through the FGFR/MAPK/NF-κB pathway in airway epithelial cells. Mil Med Res 9, 7.
[27] Fagundes, C.T., Amaral, F.A., Souza, A.L., Vieira, A.T., Xu, D., Liew, F.Y., et al., 2007. ST2, an IL-1R family member, attenuates inflammation and lethality after intestinal ischemia and reperfusion. J Leukoc Biol 81, 492–499.
[28] Zhu, W., Li, W., Jiang, J., Wang, D., Mao, X., Zhang, J., et al., 2023. Chronic salmon calcitonin exerts an antidepressant effect via modulating the p38 MAPK signaling pathway. Front Mol Neurosci 16, 1071327.
[29] Liu, J.N., Suh, D.H., Trinh, H.K., Chwae, Y.J., Park, H.S., Shin, Y.S., 2016. The role of autophagy in allergic inflammation: a new target for severe asthma. Exp Mol Med 48, e243.
[30] Shin, S., Lee, J.H., Lee, H.J., Chang, S.Y., Chung, S.H., 2018. Rapamycin attenuates Th2-driven experimental allergic conjunctivitis. Clin Immunol 190, 1–10.
[31] Chen, S., Zhou, Y., Chen, Y., Gu, J., 2018. fastp: an ultra-fast all-in-one FASTQ preprocessor. Bioinformatics 34, i884–i890.
[32] Pertea, M., Kim, D., Pertea, G.M., Leek, J.T., Salzberg, S.L., 2016. Transcript-level expression analysis of RNA-seq experiments with HISAT, StringTie and Ballgown. Nat Protoc 11, 1650–1667.
[33] Li, B., Dewey, C.N., 2011. RSEM: accurate transcript quantification from RNA-Seq data with or without a reference genome. BMC Bioinforma 12, 323.
[34] Love, M.I., Huber, W., Anders, S., 2014. Moderated estimation of fold change and dispersion for RNA-seq data with DESeq2. Genome Biol 15, 550.
[35] Xie, C., Mao, X., Huang, J., Ding, Y., Wu, J., Dong, S., et al., 2011. KOBAS 2.0: a web server for annotation and identification of enriched pathways and diseases. Nucleic Acids Res 39, W316–322.
[36] Langfelder, P., Horvath, S., 2008. WGCNA: an R package for weighted correlation network analysis. BMC Bioinforma 9, 559.
[37] Zhang, H., Qiu, S.L., Tang, Q.Y., Zhou, X., Zhang, J.Q., He, Z.Y., et al., 2019. Erythromycin suppresses neutrophil extracellular traps in smoking-related chronic pulmonary inflammation. Cell Death Dis 10, 678.
[38] Zhang, R., Sun, C., Han, Y., Huang, L., Sheng, H., Wang, J., et al., 2023. Neutrophil autophagy and NETosis in COVID-19: perspectives. Autophagy 19, 758–767.
[39] Huang, S., Wang, Y., Lin, S., Guan, W., Liang, H., Shen, J., 2023. Neutrophil autophagy induced by monosodium urate crystals facilitates neutrophil extracellular traps formation and inflammation remission in gouty arthritis. Front Endocrinol (Lausanne) 14, 1071630.
[40] Chu, C., Wang, X., Yang, C., Chen, F., Shi, L., Xu, W., et al., 2023. Neutrophil extracellular traps drive intestinal microvascular endothelial ferroptosis by impairing Fundc1-dependent mitophagy. Redox Biol 67, 102906.
[41] McInturff, A.M., Cody, M.J., Elliott, E.A., Glenn, J.W., Rowley, J.W., Rondina, M. T., et al., 2012. Mammalian target of rapamycin regulates neutrophil extracellular trap formation via induction of hypoxia-inducible factor 1 α. Blood 120, 3118–3125.
[42] Frangou, E., Chrysanthopoulou, A., Mitsios, A., Kambas, K., Arelaki, S., Angelidou, I., et al., 2019. REDD1/autophagy pathway promotes thromboinflammation and fibrosis in human systemic lupus erythematosus (SLE) through NETs decorated with tissue factor (TF) and interleukin-17A (IL-17A). Ann Rheum Dis 78, 238–248.
[43] Zhou, E., Conejeros, I., Velásquez, Z.D., Muñoz-Caro, T., Gärtner, U., Hermosilla, C., et al., 2019. Simultaneous and positively correlated NET formation

and autophagy in besnoitia besnoiti tachyzoite-exposed bovine polymorphonuclear neutrophils. Front Immunol 10, 1131.
[44] Qu, M., Chen, Z., Qiu, Z., Nan, K., Wang, Y., Shi, Y., et al., 2022. Neutrophil extracellular traps-triggered impaired autophagic flux via METTL3 underlies sepsis-associated acute lung injury. Cell Death Discov 8, 375.
[45] Li, R.H.L., Ng, G., Tablin, F., 2017. Lipopolysaccharide-induced neutrophil extracellular trap formation in canine neutrophils is dependent on histone H3 citrullination by peptidylarginine deiminase. Vet Immunol Immunopathol 193-194, 29–37.
[46] Frey, A., Lunding, L.P., Wegmann, M., 2023. The dual role of the airway epithelium in asthma: active barrier and regulator of inflammation. Cells 12, 2208.
[47] Hammad, H., Lambrecht, B.N., 2021. The basic immunology of asthma. Cell 184, 1469–1485.
[48] Konno, S., Taniguchi, N., Makita, H., Nakamaru, Y., Shimizu, K., Shijubo, N., et al., 2018. Distinct phenotypes of smokers with fixed airflow limitation identified by cluster analysis of severe asthma. Ann Am Thorac Soc 15, 33–41.
[49] Ricciardolo, F.L.M., Sprio, A.E., Baroso, A., Gallo, F., Riccardi, E., Bertolini, F., et al., 2021. Characterization of T2-Low and T2-High Asthma Phenotypes in Real-Life. Biomedicines 9, 1684.
[50] Oryszczyn, M.P., Annesi-Maesano, I., Charpin, D., Paty, E., Maccario, J., Kauffmann, F., 2000. Relationships of active and passive smoking to total ige in adults of the epidemiological study of the genetics and environment of asthma, bronchial hyperresponsiveness, and atopy (EGEA). Am J Respir Crit Care Med 161, 1241–1246.
[51] Jarvis, Deborah, Chinn, Susan, Luczynska, Christina, Burney, Peter, 1999. The association of smoking with sensitization to common environmental allergens: Results from the European community respiratory health survey. J Allergy Clin Immunol 104, 934–940.
[52] Givi, M.E., Folkerts, G., Wagenaar, G.T., Redegeld, F.A., Mortaz, E., 2015. Cigarette smoke differentially modulates dendritic cell maturation and function in time. Respir Res 16, 131.
[53] Calderon, A.A., Dimond, C., Choy, D.F., Pappu, R., Grimbaldeston, M.A., Mohan, D., et al., 2023. Targeting interleukin-33 and thymic stromal lymphopoietin pathways for novel pulmonary therapeutics in asthma and COPD. Eur Respir Rev 32, 220144.
[54] Allinne, J., Scott, G., Lim, W.K., Birchard, D., Erjefält, J.S., Sandén, C., et al., 2019. IL-33 blockade affects mediators of persistence and exacerbation in a model of chronic airway inflammation. J Allergy Clin Immunol 144, 1624–1637 e1610.
[55] Radermecker, C., Sabatel, C., Vanwinge, C., Ruscitti, C., Maréchal, P., Perin, F., et al., 2019. Locally instructed CXCR4(hi) neutrophils trigger environment-driven allergic asthma through the release of neutrophil extracellular traps. Nat Immunol 20, 1444–1455.
[56] Huang, Z., Zhang, H., Fu, X., Han, L., Zhang, H., Zhang, L., et al., 2022. Autophagy-driven neutrophil extracellular traps: The dawn of sepsis. Pathol Res Pr 234, 153896.
[57] Guzik, K., Skret, J., Smagur, J., Bzowska, M., Gajkowska, B., Scott, D.A., et al., 2011. Cigarette smoke-exposed neutrophils die unconventionally but are rapidly phagocytosed by macrophages. Cell Death Dis 2, e131.
[58] Pham, D.L., Ban, G.Y., Kim, S.H., Shin, Y.S., Ye, Y.M., Chwae, Y.J., et al., 2017. Neutrophil autophagy and extracellular DNA traps contribute to airway inflammation in severe asthma. Clin Exp Allergy 47, 57–70.
[59] Remijsen, Q., Vanden Berghe, T., Wirawan, E., Asselbergh, B., Parthoens, E., De Rycke, R., et al., 2011. Neutrophil extracellular trap cell death requires both autophagy and superoxide generation. Cell Res 21, 290–304.
[60] Chen, F., Chu, C., Wang, X., Yang, C., Deng, Y., Duan, Z., et al., 2023. Hesperetin attenuates sepsis-induced intestinal barrier injury by regulating neutrophil extracellular trap formation via the ROS/autophagy signaling pathway. Food Funct 14, 4213–4227.
[61] Chargui, A., El May, M.V., 2014. Autophagy mediates neutrophil responses to bacterial infection. Apmis 122, 1047–1058.
[62] Yazdani, H.O., Chen, H.W., Tohme, S., Tai, S., van der Windt, D.J., Loughran, P., et al., 2017. IL-33 exacerbates liver sterile inflammation by amplifying neutrophil extracellular trap formation. J Hepatol S0168 (8278), 32291–32292.
[63] Curren, B., Ahmed, T., Howard, D.R., Ashik Ullah, M., Sebina, I., Rashid, R.B., et al., 2023. IL-33-induced neutrophilic inflammation and NETosis underlie rhinovirus-triggered exacerbations of asthma. Mucosal Immunol 16, 671–684.
[64] Nian, J.B., Zeng, M., Zheng, J., Zeng, L.Y., Fu, Z., Huang, Q.J., et al., 2020. Epithelial cells expressed IL-33 to promote degranulation of mast cells through inhibition on ST2/PI3K/mTOR-mediated autophagy in allergic rhinitis. Cell Cycle 19, 1132–1142.
[65] Ng, L.G., Ostuni, R., Hidalgo, A., 2019. Heterogeneity of neutrophils. Nat Rev Immunol 19, 255–265.
[66] Khoyratty, T.E., Ai, Z., Ballesteros, I., Eames, H.L., Mathie, S., Martín-Salamanca, S., et al., 2021. Distinct transcription factor networks control neutrophil-driven inflammation. Nat Immunol 22, 1093–1106.